Synthesis and In Vivo Evaluation of Halogenated *N*,*N*-Dimethyl-2-(2′-amino-4′-hydroxymethylphenylthio)benzylamine Derivatives as PET Serotonin Transporter Ligands

Nachwa Jarkas,[†] Ronald J. Voll,[†] Larry Williams,[†] John R. Votaw,[†] Mike Owens,[‡] and Mark M. Goodman*[,†,‡]

Department of Radiology and Department of Psychiatry and Behavior Sciences, Emory University, Atlanta, Georgia 30322

Received July 3, 2007

N,*N*-Dimethyl-2-(2′-amino-4′-hydroxymethylphenylthio)benzylamine (**38**), substituted on ring A, was reported to display high binding affinity and selectivity to the human brain serotonin transporter (SERT). In an attempt to explore the potential of compounds substituted on ring B of the phenylthiophenyl core structure, three derivatives of **38** were synthesized: *N*,*N*-dimethyl-2-(2′-amino-4′-hydroxymethyl-phenylthio)-5-fluorobenzylamine (**35**), *N*,*N*-dimethyl-2-(2′-amino-4′-hydroxymethyl-phenylthio)-5-bromobenzylamine (**36**), and *N*,*N*-dimethyl-2-(2′-amino-4′-hydroxymethyl-phenylthio)-5-iodobenzylamine (**37**). The in vitro binding studies in cells transfected with human SERT, norepinephrine transporter (NET), and dopamine transporter (DAT) showed that **35**, **36**, and **37** exhibited high SERT affinity with K_is (SERT) = 1.26, 0.29, and 0.31 nM (vs [^{3}H]citalopram), respectively. [^{11}C]-(**35**), [^{11}C]-(**36**), and [^{11}C]-(**37**) were prepared by methylation of their monomethyl precursors **16**, **17**, and **18**, with [^{11}C]iodomethane in 28, 11, and 14% radiochemical yields, respectively. The microPET images of [^{11}C]-(**35**), [^{11}C]-(**36**), and [^{11}C]-(**37**) showed high uptake in the monkey brain regions rich in SERT with peak midbrain to cerebellum ratios of 3.41, 3.24, and 3.00 at 85 min post-injection, respectively. In vivo bindings of [^{11}C]-(**35**), [^{11}C]-(**36**), and [^{11}C]-(**37**) were shown to be specific to the SERT as displacement with citalopram (a potent SERT ligand) reduced radioactivity in SERT-rich regions to the cerebellum level. These results suggest that [^{11}C]-(**35**), [^{11}C]-(**36**), and [^{11}C]-(**37**) could be potential agents for mapping human SERT by PET and radiolabeling **37** with iodine-123, which could afford the first SPECT SERT imaging agent exhibiting fast kinetics.

Introduction

Depression is a chronic debilitating mental disease affecting more than 10% of the general population. The need for more effective treatment of depression continues to command attention in neuropsychopharmacology and within the psychotherapeutic community.[1] Theories on the pathophysiology of depression have emphasized deficiencies of various aspects of serotonergic transmission controlled in part by the serotonin transporter (SERT).[2] The principal function of the SERT is to terminate the action of the serotonin (indoleamine, 5-hydroxytryptamine [5-HT]) by removing it from the synaptic cleft and returning it to the presynaptic neuron where the neurotransmitter can be degraded or retained for rerelease at a later time.[3] To date, there is evidence that abnormalities in the brain central serotonin function are involved in several neuropsychiatric conditions, including major depression, anxiety, and obsessive compulsive disorder.[3] Because of the perceived importance of the brain serotonin system in these diseases, as well as a variety of normal brain functions like appetite and sleep, considerable interest has been focused on the development of functional neuroimaging techniques (e.g., positron emission tomography [PET] and single-photon emission computed tomography [SPECT]) that permit assessment of serotonin neurons in the living human brain.[4] Neuroimaging research has emerged as a valuable tool in shaping our understanding of the pathophysiology of psychiatric disorders. To this end, several laboratories have developed and evaluated various SPECT and PET radiotracers for measurements of various components of the serotonin system.[5–11] Many of these compounds from the tropane motif, except 2β-carbomethoxy-3β-(4′-((*Z*-2-iodo-ethenyl)phenyl)nortropane,[12,13] 2β-carbomethoxy-3β-(4′-((*Z*-2-iodo-ethenyl) phenyl) tropane,[14] and 2β-carbomethoxy-3β-(3′-((*Z*-2-iodo-ethenyl)phenyl)nortropane[15] have failed to show promising imaging properties in the nonhuman primate and human brain. The most common limitation has been a combination of deficient selectivity, inappropriate kinetics, and inadequate in vivo binding specificity.

In the past few years, there has been considerable interest in the phenylthiophenyl core structure of the serotonin reuptake inhibitor 403U76 (Figure 1)[16] that led to a new class of compounds: the substituted diaryl sulfides. From this same class, a large collection of carbon-11, fluorine-18,[17–20] and iodine-123[21,22] labeled radioligands have been synthesized and evaluated as potential PET and SPECT SERT imaging agents. The carbon-11 radiotracers included [^{11}C]-(**38**),[23,24] [^{11}C]-(**39**),[23,25] [^{11}C]-(**40**),[26–28] ([^{11}C]-(**40**) is ^{11}C-DASB, a well established PET SERT imaging agent widely used) [^{11}C]-(**41**),[26] [^{11}C]-(**42**),[23,29,30] [^{11}C]-(**43**),[27,31] [^{11}C]-(**44**),[27] [^{11}C]-(**45**),[27,32] [^{11}C]-(**46**),[33] and [^{11}C]-(**47**)[34] (Figure 1). Radiolabeled with iodine-123, **44** was reported to bind selectively to the human brain SERT.[35–37] However, this radioligand exhibited slow brain kinetics, reaching a near steady state 3 h after tracer injection.[37] In our laboratory, preclinical studies indicated that [^{11}C]-(**38**) exhibited high affinity and selectivity for the SERT in vitro and that, in vivo, it showed selective binding to the SERT in the regions of interest of a rhesus monkey brain.[24] Furthermore, [^{11}C]-(**38**) displayed better tissue-to-cerebellum ratios relative to [^{11}C]-(**40**) and an earlier time to reach maximal uptake relative to [^{11}C]-(**45**).[24] Also, low

* To whom correspondence should be addressed. Mark M. Goodman, Ph.D., Emory University, School of Medicine, Department of Radiology, 1364 Clifton Road, NE, Atlanta, GA 30322. Phone: (404) 727-9366. Fax: (404) 727-3488. E-mail: mgoodma@emory.edu.

[†] Department of Radiology.

[‡] Department of Psychiatry and Behavior Sciences.

10.1021/jm0707929 CCC: $40.75
Published on Web 12/18/2007

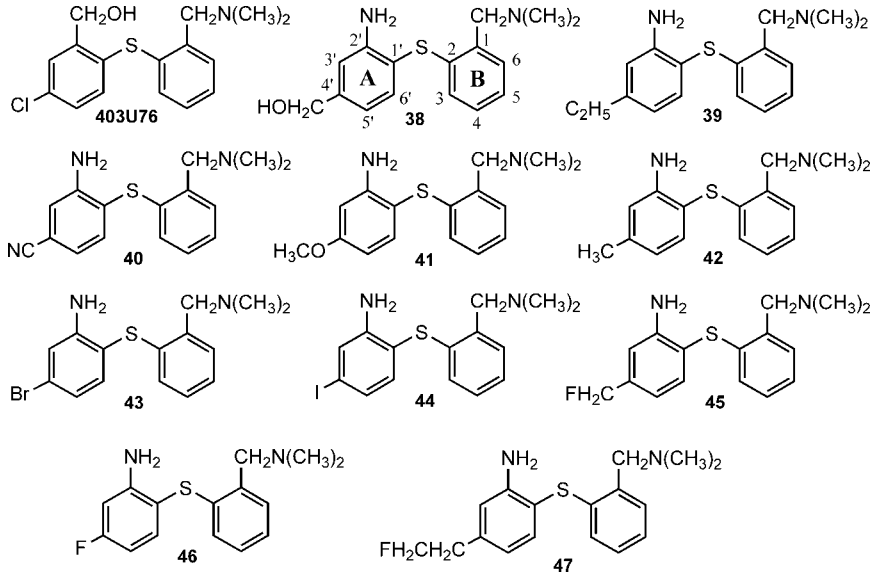

Figure 1. Substituted diaryl sulfide compounds.

Scheme 1. Synthesis of 5-Iodo-2-mercaptobenzoic Acid (**6**)[a]

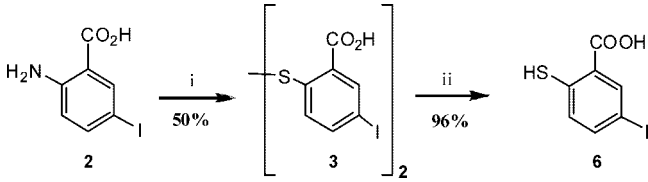

[a] Conditions: (i) H_2O, HCl, $NaNO_2$, Na_2S_2; (ii) $NaBH_4$, THF, 0 °C to rt, 15 min.

concentrations of radioactive metabolites in arterial plasma samples of rhesus monkey blood, relative to the parent compound, suggested that this radioligand holds significant potential for use in evaluating the status of the SERT in clinical settings. Indeed, it has since advanced to imaging applications in humans.[38] Most of the diaryl sulfides reported are derivatives having substitutions on phenyl ring A. Recently, few derivatives of the diaryl sulfide class with substitutions on phenyl ring B have been reported.[39] The 4′-iodo-biphenylthiol derivative peaked at 6–12 h after tracer injection, which might be too slow for SPECT imaging.

The desire of further exploring the potential of compounds substituted on ring B and the interesting results shown by **38** prompted us to think about incorporating a halogen atom (F, Br, and I) onto the 5-position of ring B of the phenylthiophenyl structure of **38** (Figure 1). In this paper, we report the synthesis, radiolabeling, pharmacological characterization, and microPET imaging studies, in cynomolgus monkeys, of **35**, **36**, and **37**, three halogeno-derivative compounds of **38**.

Results and Discussion

Chemistry. The synthesis of the new target ligands *N*,*N*-dimethyl-2-(2′-amino-4′-hydroxymethyl-phenylthio)-5-fluorobenzylamine (**35**), *N*,*N*-dimethyl-2-(2′-amino-4′-hydroxymethyl-phenylthio)-5-bromobenzylamine (**36**), and *N*,*N*-dimethyl-2-(2′-amino-4′-hydroxymethyl-phenylthio)-5-iodobenzylamine (**37**; Scheme 3), as well as the monomethyl derivatives *N*-methyl-2-(2′-amino-4′-hydroxymethylphenylthio)-5-fluoro-benzylamine (**16**), *N*-methyl-2-(2′-amino-4′-hydroxymethylphenylthio)-5-bromo-benzylamine (**17**), and *N*-methyl-2-(2′-amino-4′-hydroxymethylphenylthio)-5-iodo-benzylamine (**18**; Scheme 2), required as precursors for radiolabeling with [^{11}C]iodomethane, is presented in Schemes 1−3. Compounds **2**, **4**, **5**, and **19** were commercially available. Compound **1**[24] was prepared from 4-bromo-3-nitro-toluene (**19**) using previously described procedures.[24] Diazotization[40] of 2-amino-5-iodobenzoic acid (**2**) followed by a reaction with sodium disulfide, gave 2,2′-dithiobis-(5-iodobenzoic) acid (**3**; Scheme 1). Disulfide (**3**) was reduced with sodium borohydride in anhydrous tetrahydrofuran to give the 5-iodo-2-mercaptobenzoic acid (**6**) in very good yield (Scheme 1).

The synthesis of fluoro-, bromo-, and iodo-monomethylamines **16**, **17**, and **18** was initiated by the coupling[41] of **1**[24] with thiosalicylic acids **4**, **5**, and **6** to afford **7**, **8**, and **9**, respectively, in good yields (Scheme 2). Treatment of **7**, **8**, and **9** with thionyl chloride in refluxing dichloromethane (DCM) and a catalytic amount of dimethylformamide (DMF) gave the crude acid chlorides, which were reacted, without further purification, with methylamine hydrochloride in anhydrous dichloromethane to yield the desired monomethylbenzamides **10**, **11**, and **12**, respectively, in low yields (Scheme 2). Reduction of the amide and acetoxy groups of **10**, **11**, and **12** with the diborane-tetrahydrofuran (1 M) complex provided **13**, **14**, and **15**, which, after reduction of the nitro group with tin chloride, were transformed to **16**, **17**, and **18**, respectively.

Under the same reaction conditions used to prepare **7**, **8**, and **9**, condensation of **19** with thiosalicylic acids **4**, **5**, and **6** proceeded smoothly in dimethylformamide, yielding **20**, **21**, and **22**, respectively, which, under the appropriate conditions, were converted to dimethylbenzamides **23**, **24**, and **25** (Scheme 3). Radical bromination with *N*-bromosuccinimide of **23**, **24**, and **25** proceeded smoothly in carbon tetrachloride,[42] yielding **26**, **27**, and **28**, which were subsequently transformed to **29**, **30**, and **31** by nucleophilic substitution with potassium acetate. The target compounds **35**, **36**, and **37** were obtained from **29**, **30**, and **31**, respectively, following the same conditions used to prepare **16**, **17**, and **18** (Scheme 3).

Radiochemistry. The labeling of [^{11}C]-(**35**), [^{11}C]-(**36**), and [^{11}C]-(**37**) was accomplished by alkylation of precursors **16**, **17**, and **18** with [^{11}C]iodomethane, as depicted in Scheme 4. The monomethylbenzylamines **16**, **17**, and **18** reacted with cyclotron produced [^{11}C]iodomethane, at room temperature for 5 min, on a standard High Performance Liquid Chromatography (HPLC) loop injector in a manner similar to the previously

Scheme 2. Synthesis of the Monomethyl Precursors **16**, **17**, and **18**[a]

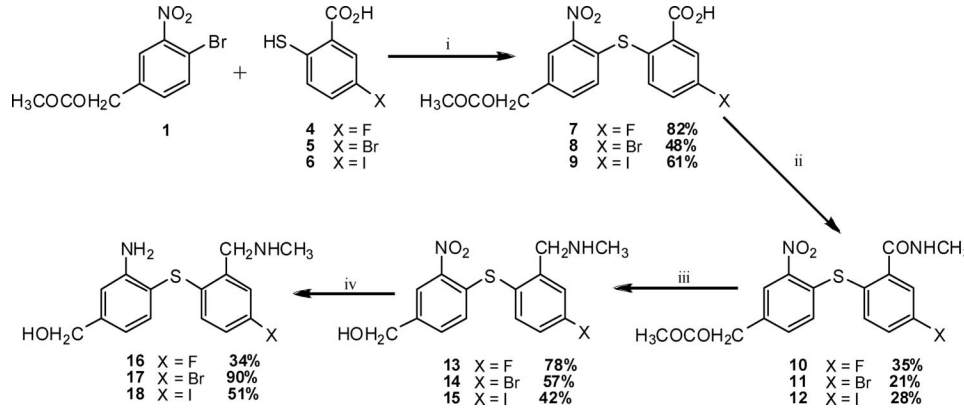

[a] Conditions: (i) K_2CO_3, DMF, 130 °C; (ii) 1-$SOCl_2$, DCM, reflux; 2-DCM/Et_3N, CH_3NH_2, HCl, −70 °C; (iii) BH_3-THF, reflux, 5 h, rt, 18 h; (iv) $SnCl_2$, cc.HCl/CH_3OH, 0 °C to rt.

Scheme 3. Synthesis of the Target *N*,*N*-Dimethyl Benzylamines **35**, **36**, and **37**[a]

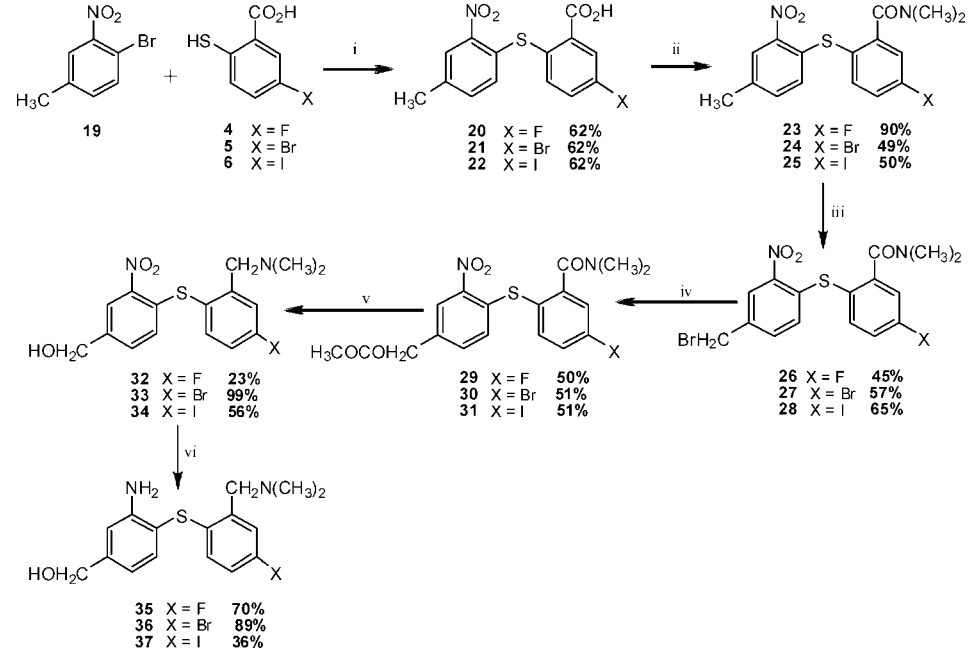

[a] Conditions: (i) K_2CO_3, DMF, 130 °C; (ii) 1-$SOCl_2$, DCM, reflux; 2-$(CH_3)_2NH$/THF, −70 °C; (iii) NBS, AIBN, CCl_4, reflux; (iv) CH_3CO_2K, DMF; (v) BH_3-THF, reflux, 5 h, rt, 18 h; (vi) $SnCl_2$, cc.HCl/CH_3OH, 0 °C to rt.

Scheme 4. Synthesis of [^{11}C]-(**35**), [^{11}C]-(**36**), and [^{11}C]-(**37**)

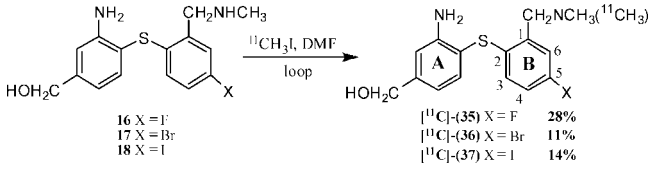

reported "loop method".[43] [^{11}C]-(**35**), [^{11}C]-(**36**), and [^{11}C]-(**37**) were purified by reversed-phase HPLC. For in vivo studies, the HPLC fractions containing [^{11}C]-(**35**) were combined and the desired product was formulated in 10% ethanol in saline using a C_{18} solid-phase-extraction cartridge.[24,44] [^{11}C]-(**36**) and [^{11}C]-(**37**) were formulated in a similar manner. The entire labeling, purification, and formulation procedure required approximately 45 min from end of bombardment. [^{11}C]-(**35**), [^{11}C]-(**36**), and [^{11}C]-(**37**) were prepared with a specific activity of 1550 ± 610 mCi/μ mol (n = 3), 750 ± 320 mCi/μ mol (n = 3), and 663 ± 350 mCi/μ mol (n = 3; at time of injection), in 28 ± 13% (n = 3), 11 ± 4% (n = 3), and 14 ± 5% (n = 3), respectively, decay-corrected radiochemical yield (based on [^{11}C]iodomethane production). The yields are for final formulated products, corrected for decay and normalized for a 60 min (40 μA) bombardment that produces approximately 500 mCi of [^{11}C]iodomethane from the GE MicroLab methyl iodide system. The amount of radioactivity formed (500 mCi) was measured by trapping the [^{11}C]iodomethane released in 200 μL of DMF in a sealed vial immersed in an ice/water bath. Analytical HPLC showed that the labeled products [^{11}C]-(**35**), [^{11}C]-(**36**), and [^{11}C]-(**37**) had chemical and radiochemical purities of >99%. The lipophilicities (n-octanol/0.02 M phosphate buffer partition) (log $P_{7.4}$) of these radiotracers were measured[24,25] and are presented in Table 1. Log $P_{7.4}$ is an important parameter for correlating structure with brain penetrance and ligand-transporter kinetic behavior. [^{11}C]-(**35**), [^{11}C]-(**36**), and [^{11}C]-(**37**) had log $P_{7.4}$ values of 2.06, 2.63, and 1.82, respectively (Table 1). [^{11}C]-(**37**) (1.82) exhibited lower log $P_{7.4}$ than [^{11}C]-(**35**) (2.06), and [^{11}C]-(**37**) (2.63). Comparison between the parent 5-unsubstituted compound **38** and the 5-halogeno-substituted compounds **35**, **36**, and **37** demonstrated that a halogen (F, Br, and I)

Table 1. Binding Affinities (K_i (nM)) of Candidate SERT Ligands in Cells Expressing Human Transporters and Lipophilicities (log $P_{7.4}$)

cmpd	SERT[a] (*n*)[b]	DAT[c] (*n*)	NET[d] (*n*)	log $P_{7.4}$	DAT/SERT	NET/SERT
35	1.26 ± 0.06 (2)	>2000 (2)	618 ± 120 (2)	2.06 ± 0.03	>1000	490
36	0.29 ± 0.01 (3)	221 ± 18 (2)	725 ± 30 (2)	2.63 ± 0.2	762	>2000
37	0.31 ± 0.02 (2)	>2000 (2)	467 ± 29 (2)	1.82 ± 0.1	>1000	>1000
38[24]	0.57 ± 0.05 (3)	>1000 (3)	303 ± 226 (3)	1.60 ± 0.01	>1000	532

[a] Competitive binding versus [^{3}H]citalopram in human kidney cells transfected with human serotonin transporters. [b] Number of assays. Values were obtained from the mean ± SD of at least two independent assays each in duplicates. [c] Competitive binding versus [^{125}I]RTI-55 in canine kidney cells transfected with human dopamine transporters. [d] Competitive binding versus [^{3}H]nisoxetine in human kidney cells transfected with human norepinephrine transporters.

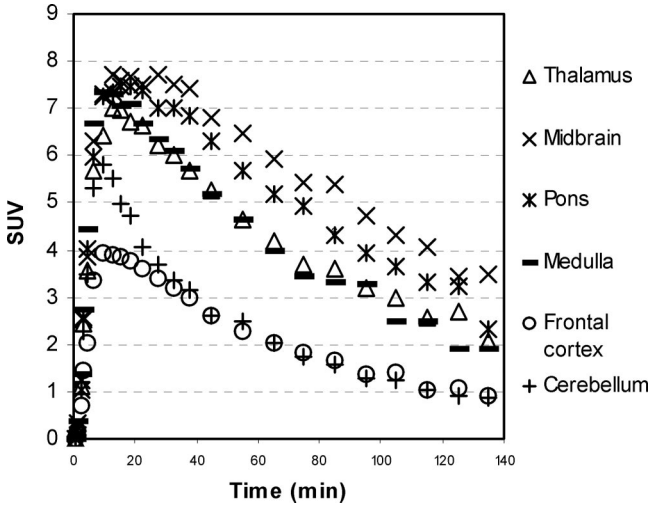

Figure 2. MicroPET time−activity curves of a male cynomolgus monkey brain regions, thalamus, midbrain, pons, medulla, frontal cortex, and cerebellum after i.v. injection of 15.26 mCi of [^{11}C]-(**35**).

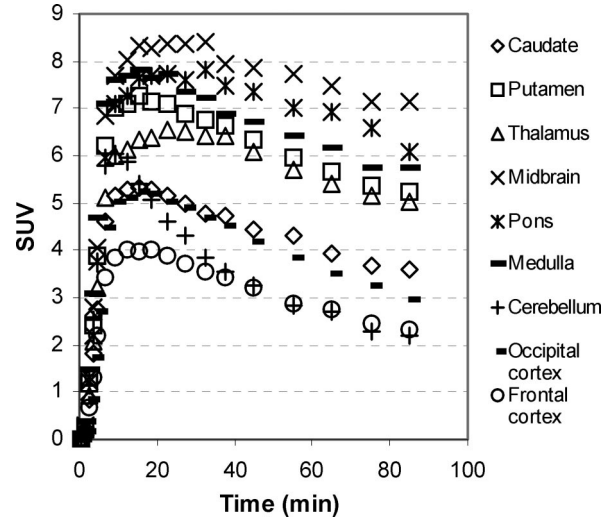

Figure 3. MicroPET time−activity curves of a male cynomolgus monkey brain regions, caudate, putamen, thalamus, midbrain, pons, medulla, cerebellum, occipital cortex, and frontal cortex after i.v. injection of 11.36 mCi of [^{11}C]-(**36**).

increased log $P_{7.4}$ by 0.22–1.03. Furthermore, the 1.82 value of [^{11}C]-(**37**) was most similar to the measured value of 1.60 of **38** (Table 1), which achieved brain penetrance and good specific (midbrain) to nonspecific binding (cerebellum) ratios greater than 4.[24]

In Vitro Competition Assays. The affinities of *N*,*N*-dimethyl derivatives **35**, **36**, and **37** for the human SERT (hSERT), human DAT (hDAT), and human NET (hNET) were determined through in vitro competition assays according to a known procedure previously reported.[23] These data are shown in Table 1 along with the previously determined K_i values of **38**.[24] The data in Table 1 showed that **35**, **36**, and **37** displayed high affinity and selectivity for the SERT over the DAT and NET. The rank of order of hSERT affinity (K_i in nM) was **36** (0.29) > **37** (0.31) > **38** (0.57)[24] > **35** (1.26). Furthermore, **35**, **36**, and **37** exhibited low affinities for the hDAT and hNET (K_i > 200 nM; Table 1). These findings demonstrated that the incorporation of a halogen (F, Br, and I) onto the 5-position of ring B of the diphenyl sulfide structure of **38** resulted in minor changes in the binding potency to the SERT.

MicroPET Nonhuman Primate Imaging. The regional brain distribution of [^{11}C]-(**35**), [^{11}C]-(**36**), and [^{11}C]-(**37**) was determined in an anesthetized male cynomolgus monkey using a Concorde MicroPET P4. MicroPET imaging studies were performed to determine the uptake of [^{11}C]-(**35**), [^{11}C]-(**36**), and [^{11}C]-(**37**) in the brain regions rich in SERT. The regional distribution of radioactivity in the brain following administration of [^{11}C]-(**35**), [^{11}C]-(**36**), and [^{11}C]-(**37**) showed the highest uptake in the midbrain such as hypothalamus, a region where the SERT density is high, whereas the lowest uptake was detected in the SERT poor cerebellum (Figures 2, 3, 4, and 5).

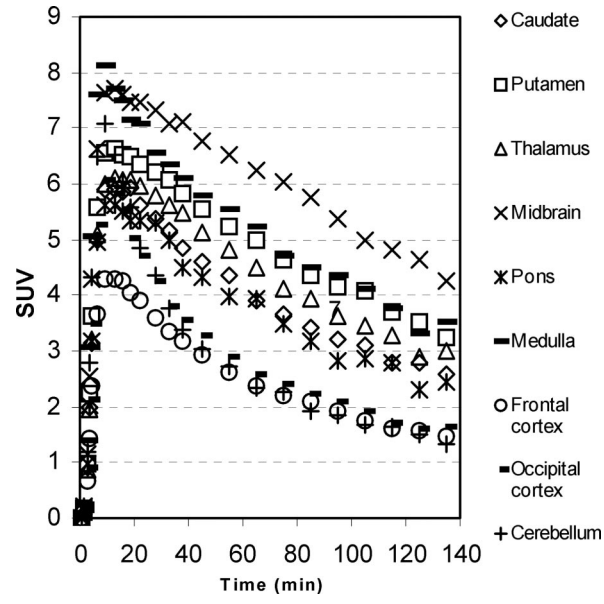

Figure 4. MicroPET time−activity curves of a male cynomolgus monkey brain regions, caudate, putamen, thalamus, midbrain, pons, medulla, frontal cortex, occipital cortex, and cerebellum after i.v. injection of 18.20 mCi of [^{11}C]-(**37**).

MicroPET time−activity curves for the thalamus, midbrain, pons, medulla, frontal cortex, and cerebellum in a cynomolgus monkey after [^{11}C]-(**35**) injection are presented in Figure 2. Following administration of [^{11}C]-(**35**), the rank of order of uptake of radioactivity in the cynomolgus monkey brain was midbrain > pons > thalamus ∼ medulla, regions rich with

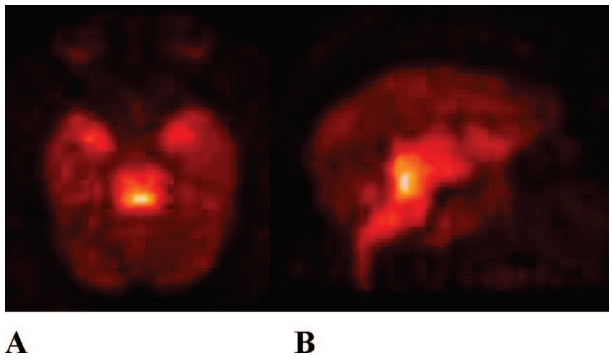

Figure 5. Summed (0–120 min) transaxial (**A**), and sagittal (**B**) images from microPET acquisitions in a male cynomolgus monkey after i.v. injection of 18.20 mCi of [^{11}C]-(**37**).

Table 2. Region-of-Interest to Cerebellum Activity Ratios at 85 min after Injection of [^{11}C]-(**35**), [^{11}C]-(**36**), and [^{11}C]-(**37**)

region	[^{11}C]-(**35**)	[^{11}C]-(**36**)	[^{11}C]-(**37**)
caudate		1.70	1.80
putamen		2.40	2.30
thalamus	2.30	2.30	2.06
midbrain	3.40	3.24	3.00
pons	2.80	2.80	1.65
medulla	2.10	2.60	2.40
occipital cortex		1.34	1.20
frontal cortex	1.04	1.06	1.09

SERT. Lower uptake was measured in the frontal cortex, whereas the lowest uptake was detected in the cerebellum (Figure 2). Surprisingly, the caudate and putamen regions were not readily visible and could not be included in Figure 2. The regional distribution of radioactivity in the brain following administration of [^{11}C]-(**35**) was consistent with binding to SERT-rich sites (Figure 2). The peak uptake of radioactivity in the midbrain occurred between 12.5 and 27.5 min after injection and then declined with a $T_{1/2} = 90$ min. The brain regions of interest (ROIs) to cerebellum ratios at 85 min after [^{11}C]-(**35**) injection are presented in Table 2.

Figure 3 shows the time−activity curves obtained after injection of [^{11}C]-(**36**) into a cynomolgus monkey. The uptake of radioactivity occurred in the following order: midbrain > pons > medulla > putamen > thalamus > caudate. The caudate and putamen regions are rich with both DAT and SERT. Lower uptake was measured in the occipital cortex and frontal cortex, whereas the lowest uptake was observed in the cerebellum (Figure 3). The peak uptake of radioactivity in the midbrain was achieved between 15.5 and 32.5 min and then declined slowly. The brain regions of interest to cerebellum ratios at 85 min after [^{11}C]-(**36**) injection are presented in Table 2.

The regional distribution of radioactivity in the brain of a cynomolgus monkey following administration of [^{11}C]-(**37**) is depicted in the time−activity curves for brain ROIs (Figure 4). The rank order of uptake of radioactivity in the cynomolgus brain was midbrain > medulla ∼ putamen > thalamus > pons ∼ caudate. Lower uptake was observed in the occipital cortex and frontal cortex. The lowest uptake occurred in the cerebellum (Figure 4). The radioactivity uptake in the midbrain peaked between 12.5 and 22.5 min and then declined with a $T_{1/2} = 90$ min. The brain regions of interest to cerebellum ratios at 85 min after [^{11}C]-(**37**) injection are presented in Table 2. The summed microPET images acquired from 0 to 120 min in a male cynomolgus monkey following [^{11}C]-(**37**) accumulation in the midbrain are shown in Figure 5.

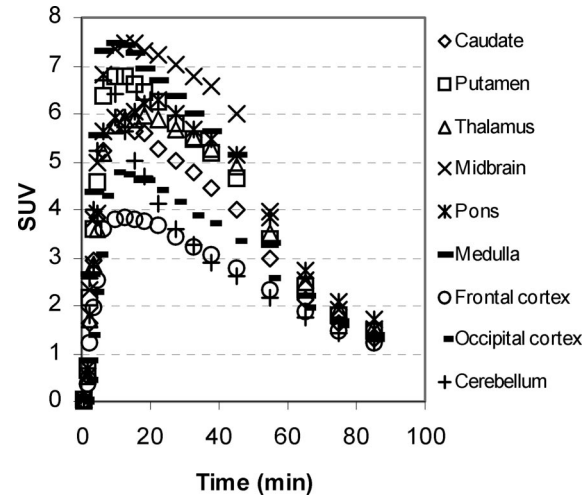

Figure 6. MicroPET time−activity curves of a male cynomolgus monkey brain regions, caudate, putamen, thalamus, midbrain, pons, medulla, frontal cortex, occipital cortex, and cerebellum after i.v. injection of 18.10 mCi of [^{11}C]-(**35**). Citalopram (1.5 mg/kg body weight) was administered at 45 min post-injection of [^{11}C]-(**35**).

These small differences in the uptake of radioactivity in the cynomolgus monkey brain between [^{11}C]-(**35**), [^{11}C]-(**36**), and [^{11}C]-(**37**) in comparison to [^{11}C]-(**38**) suggest that the hydroxylmethyl substituent on the 4-position of ring A of the biphenylthiol motif has the dominant influence on SERT binding. The faster binding kinetics exhibited by [^{11}C]-(**35**) in comparison to [^{11}C]-(**36**) and [^{11}C]-(**37**) may reflect a lower binding affinity to the SERT (Table 1). Furthermore, the lower midbrain-to-cerebellum ratios, at 85 min, of [^{11}C]-(**35**) (3.41), [^{11}C]-(**36**) (3.24), and [^{11}C]-(**37**) (3.00; Table 2) and the slower kinetics relative to [^{11}C]-(**38**) (3.70∼4.00)[24] at the same time may be explained in part by the fact that [^{11}C]-(**35**), [^{11}C]-(**36**), and [^{11}C]-(**37**) have higher log $P_{7.4}$ values, 2.06, 2.63, and 1.82, respectively, than [^{11}C]-(**38**) (1.60; Table 1). Furthermore, for [^{11}C]-(**37**), the uptake kinetics, peaking between 12.5 and 22.5 min, may serve for translation of **37** to SPECT imaging when labeled with iodine-123. [^{123}I]-(**37**) has the potential to be the first example of an iodinated radioligand with fast kinetics, based on the biphenylthiol core structure, to image the SERT by SPECT.

To demonstrate that the brain regional [^{11}C]-(**35**), [^{11}C]-(**36**), and [^{11}C]-(**37**) binding was specific to the SERT, in vivo microPET displacement studies by the SERT ligand *R*,*S*-citalopram·HBr were performed on the same male cynomolgus monkey. A dose (1.5 mg/kg body weight) of *R*,*S*-citalopram·HBr was administered intravenously at 45 min post [^{11}C]-(**35**) and at 60 min post [^{11}C]-(**36**) and [^{11}C]-(**37**) and resulted in a significant reduction of radioactivity in the SERT-rich brain regions, caudate, putamen, thalamus, midbrain, pons, medulla, frontal cortex, and occipital cortex, while the uptake in the cerebellum was not affected (Figures 6, 7, and 8).

The reduction in the tissue-to-cerebellum ratios of [^{11}C]-(**35**), [^{11}C]-(**36**), and [^{11}C]-(**37**) in the regions of interest of the chase scan before (at 45 min for [^{11}C]-(**35**) and at 55 min for [^{11}C]-(**36**) and [^{11}C]-(**37**)) and after (at 85 min for [^{11}C]-(**35**) and (at 115 min for [^{11}C]-(**36**) and [^{11}C]-(**37**)) citalopram administration (Table 3) indicated that regional [^{11}C]-(**35**), [^{11}C]-(**36**), and [^{11}C]-(**37**) uptake reflected specific SERT binding.

Conclusion

A halogen (F, Br, and I) was incorporated onto the 5-position of phenyl ring B of the diphenyl sulfide core structure of **38** to

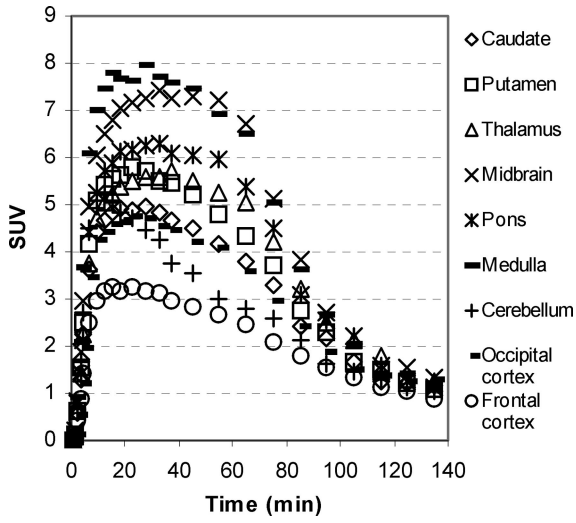

Figure 7. MicroPET time−activity curves of a male cynomolgus monkey brain regions, caudate, putamen, thalamus, midbrain, pons, medulla, cerebellum, occipital cortex, and frontal cortex after i.v. injection of 6.90 mCi of [^{11}C]-(**36**). Citalopram (1.5 mg/kg body weight) was administered at 60 min post-injection of [^{11}C]-(**36**).

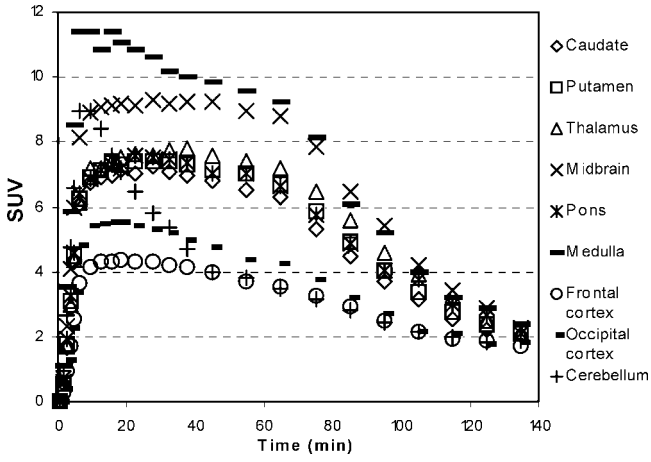

Figure 8. MicroPET time−activity curves of a male cynomolgus monkey brain regions, caudate, putamen, thalamus, midbrain, pons, medulla, frontal cortex, occipital cortex, and cerebellum after i.v. injection of 8.97 mCi of [^{11}C]-(**37**). Citalopram (1.5 mg/kg body weight) was administered at 60 min post-injection of [^{11}C]-(**37**).

Table 3. Region-of-Interest to Cerebellum Activity Ratios Post-Injection of [^{11}C]-(**35**), [^{11}C]-(**36**), and [^{11}C]-(**37**) Before and After Citalopram Administration

region	[^{11}C]-(**35**) at 45 min (85 min)	[^{11}C]-(**36**) at 55 min (115 min)	[^{11}C]-(**37**) at 55 min (115 min)
caudate	1.60 (1.06)	1.40 (1.00)	1.80 (1.30)
putamen	1.80 (1.20)	1.60 (1.20)	1.90 (1.40)
thalamus	1.90 (1.30)	1.80 (1.40)	2.00 (1.63)
midbrain	2.30 (1.20)	2.40 (1.20)	2.40 (1.70)
pons	2.00 (1.40)	2.00 (1.23)	1.90 (1.50)
medulla	2.00 (1.10)	2.30 (1.10)	2.50 (1.60)
occipital cortex	1.30 (1.04)	1.35 (1.10)	1.20 (1.10)
frontal cortex	1.06 (1.00)	1.00 (1.00)	1.00 (1.00)

give the fluoro-, bromo-, and iodo-diphenyl sulfides **35**, **36**, and **37**, respectively. In vitro and in vivo studies demonstrated that the three carbon-11-labeled compounds were selective and potent radioligands suitable to image the SERT by PET. In vivo microPET imaging studies in a male cynomolgus monkey showed that [^{11}C]-(**35**), [^{11}C]-(**36**), and [^{11}C]-(**37**) displayed high uptake in the midbrain, thalamus, pons, medulla, caudate, putamen (except for [^{11}C]-(**35**), where the caudate and putamen were not visible in the PET images), and cortical regions of the brain, with a peak uptake established around 12–27 min. Citalopram chase studies with [^{11}C]-(**35**), [^{11}C]-(**36**), and [^{11}C]-(**37**) confirmed the binding of these radiotracers to the monkey brain SERT. Furthermore, the current data also suggested that [^{11}C]-(**37**) has attractive kinetic characteristics as a PET SERT ligand when radiolabled with carbon-11, and when radiolabeled with iodine-123, this radiotracer may serve as the first candidate of the diphenyl sulfide series, with fast kinetics, to image the SERT in vivo by SPECT.

Experimental Section

Proton nuclear magnetic resonance (NMR) spectra were run on a Varian Unity 400 at 400 MHz (^{1}H) in $CDCl_3$ with tetramethylsilane (TMS) as internal standard. Elemental analyses were performed by Atlantic Microlabs, Inc. (Atlanta, GA) and were within ±0.4% of theoretical values. Compound **1**[24] was prepared and purified by methods previously reported.[24] All other chemicals were purchased from Aldrich Chemical Co. and were used without further purification. Purification and analyses of radioactive compounds by HPLC were performed with in-line UV (254 nm) detectors in series with a radioactivity detector. The HPLC columns used were either a Waters XTerra C_{18} reverse phase (19 × 100 mm; column A) for purification or a Waters C_{18} reverse phase (3.9 × 150 mm; column B) for quality control.

2,2′-Dithiobis(5-iodobenzoic) Acid (3). A solution of 2-amino-5-iodobenzoic acid (**2**; 10.00 g, 38.00 mmol) in a mixture of water (76 mL) and concentrated hydrochloric acid (cc. HCl; 13 mL) was diazotized at 0 °C with a solution of sodium nitrite ($NaNO_2$; 4.50 g, 65.22 mmol) in water (25 mL) added dropwise. The solution was stirred 1 h at 0 °C and then added to a solution of Na_2S_2 [prepared by heating sodium sulfide·nonahydrate ($Na_2S·9H_2O$; 16.70 g, 69.53 mmol) and S (2.20 g, 68.62 mmol) in water (200 mL), treating the yellow clear solution with NaOH (2.50 g, 62.50 mmol) in water (20 mL) and cooling] containing ice. The mixture was allowed to stand for 3 h at room temperature and acidified with cc. HCl, and the precipitated crude product was filtered. It was dissolved in a warm solution of Na_2CO_3 and filtered with charcoal through celite, and the filtrate was acidified again with cc. HCl. The precipitated product was filtered, washed with water, and dried: orange solid (10.58 g, 50%). It was used in the next step without further purification.

5-Iodo-2-mercaptobenzoic Acid (6). To a 50 mL, round-bottom flask capped with a rubber septum was added anhydrous tetrahydrofuran (THF; 7 mL) under argon (g). To this was added **3** (1.00 g, 1.79 mmol) to give a yellow solution of the disulfide in the solvent. The flask was immersed in an ice/water bath. To the reaction mixture was slowly and portionwise added sodium borohydride ($NaBH_4$; 0.27 g, 7.17 mmol). The color of the mixture turned to red-brown immediately after addition of the hydride reagent and the mixture became homogeneous. After 15 min, the reaction was quenched with cold water and acidified with cc. HCl. The precipitated product was filtered, washed with water, and dried to give the desired thiol (**6**) as a light yellow solid. (0.48 g, 96%). ^{1}H NMR ($CDCl_3$, δ): 4.66 (s, 1H, SH), 7.08 (d, 1H, J = 8.0 Hz, ArH), 7.64 (dd, 1H, J = 2.0, 8.0 Hz, ArH), 8.42 (d, 1H, J = 1.6 Hz, ArH). MS m/z 278.90 $(M - H)^+$.

2-(4′-Acetoxymethyl-2′-nitrophenylthio)-5-fluorobenzoic Acid (7). To a solution of **1** (0.30 g, 1.09 mmol) in DMF (7 mL) was added fluorothiosalicylic acid (**4**; 0.19 g, 1.09 mmol) followed by K_2CO_3 (0.45 g, 3.28 mmol). The reaction mixture was stirred at 130 °C for 18 h. After cooling down to room temperature, the reaction mixture was poured into cold water and extracted with ethylacetate (EtOAc). Aqueous layers were acidified with concd HCl and extracted with EtOAc. Organic layers were washed with water, dried over Na_2SO_4, and concentrated under reduced pressure to give the crude product as a yellow solid. Purification by silica

gel flash column chromatography (DCM/MeOH: 9/1) afforded **7** as an orange oil (0.33 g, 82%). ^{1}H NMR ($CDCl_3$, δ): 2.12 (s, 3H, $COCH_3$), 5.11 (s, 2H, CH_2O), 6.92 (d, 1H, J = 8.0 Hz, ArH), 7.29 (m, 1H, ArH), 7.37 (dd, 1H, J = 2.0, 8.4 Hz, ArH), 7.53 (m, 1H, ArH), 7.77 (dd, 1H, J = 2.8, 8.8 Hz, ArH), 8.17 (d, 1H, J = 1.6 Hz, ArH).

2-(4′-Acetoxymethyl-2′-nitrophenylthio)-5-bromobenzoic Acid (8). Compound **8** was prepared by the method described for **7**, by condensation of **1** (3.18 g, 11.61 mmol) with **5** (2.00 g, 11.61 mmol) in DMF (20 mL) in the presence of K_2CO_3 (4.82 g, 34.85 mmol) as a base. Silica gel flash column chromatography purification (DCM/MeOH: 9/1) afforded **8** as an orange oil (2.37 g, 48%). ^{1}H NMR ($CDCl_3$, δ): 2.11 (s, 3H, $COCH_3$), 5.13 (s, 2H, CH_2O), 7.06 (d, 1H, J = 8.4 Hz, ArH), 7.16 (d, 1H, J = 8.4 Hz, ArH), 7.31 (dd, 1H, J = 2.0, 8.4 Hz, ArH), 7.55 (dd, 1H, J = 2.4, 8.8 Hz, ArH), 7.88 (d, 1H, J = 1.2 Hz, ArH), 8.21 (d, 1H, J = 2.4 Hz, ArH).

2-(4′-Acetoxymethyl-2′-nitrophenylthio)-5-iodobenzoic Acid (9). Compound **9** was prepared by the method described for **7**, by condensation of **1** (0.20 g, 0.73 mmol) with **6** (0.20 g, 0.73 mmol) in DMF (5 mL) in the presence of K_2CO_3 (0.30 g, 2.19 mmol) as a base. Silica gel flash column chromatography purification (DCM/MeOH: 9/1) afforded **9** as an orange solid (0.21 g, 61%). ^{1}H NMR ($CDCl_3$, δ): 2.13 (s, 3H, $COCH_3$), 5.13 (s, 2H, CH_2O), 7.03 (d, 1H, J = 8.8 Hz, ArH), 7.19 (d, 1H, J = 8.0 Hz, ArH), 7.45 (m, 2H, ArH), 7.90 (d, 1H, J = 1.2 Hz, ArH), 8.19 (d, 1H, J = 2.4 Hz, ArH).

***N*-Methyl-2-(5′-acetoxymethyl-2′-nitrophenylthio)-5-fluorobenzamide (10).** To a suspension of **7** (0.31 g, 0.85 mmol) in anhydrous DCM (8 mL) were added thionyl chloride (0.25 g, 2.12 mmol) and a few drops of DMF. The reaction mixture was refluxed for 90 min under argon. The solvent was evaporated and the solid was used without further purification.

A solution of triethylamine (0.67 g, 6.67 mmol) and methylamine hydrochloride (0.22 g, 3.33 mmol) in anhydrous DCM (10 mL) was cooled down to −70 °C. The acid chloride (0.32 g, 0.85 mmol; freshly prepared) in DCM (5 mL) was added dropwise under argon. The reaction mixture was allowed to warm up to room temperature, stirred for 30 min, and mixed with cold water. The organic phase was washed with saturated Na_2CO_3 solution followed by water, and the resulting organic layers were combined, dried over Na_2SO_4, and concentrated under reduced pressure. The product was purified by silica gel flash column chromatography (DCM/EtOAc: 8/2) to yield **10** as a yellow oil (0.11 g, 35%). ^{1}H NMR ($CDCl_3$, δ): 2.11 (s, 3H, $COCH_3$), 2.87 (d, 3H, NCH_3), 5.08 (s, 2H, CH_2O), 6.37 (s, 1H, NH), 6.83 (d, 1H, J = 8.4 Hz, ArH), 7.23 (m, 1H, ArH), 7.37 (dd, 1H, J = 1.6, 8.0 Hz, ArH), 7.52 (dd, 1H, J = 2.8, 8.4 Hz, ArH), 7.61 (m, 1H, ArH), 8.22 (d, 1H, J = 2.0 Hz, ArH). Anal. ($C_{17}H_{15}FN_2O_5S$) C, H, N.

***N*-Methyl-2-(5′-acetoxymethyl-2′-nitrophenylthio)-5-bromobenzamide (11).** Acid **8** (0.20 g, 0.47 mmol) was treated with thionyl chloride (0.14 g, 1.17 mmol), as described for **10**. The crude acid chloride (0.21 g, 0.47 mmol; freshly prepared) in DCM (10 mL) was treated with methylamine hydrochloride (0.13 g, 1.89 mmol) in the presence of triethylamine (0.38 g, 3.77 mmol). The methylamide derivative (**11**) was purified by silica gel flash column chromatography (DCM/EtOAc: 8/2) to give a yellow oil (44.0 mg, 21%). ^{1}H NMR ($CDCl_3$, δ): 2.09 (s, 3H, $COCH_3$), 2.83 (d, 3H, NCH_3), 5.07 (s, 2H, CH_2O), 6.39 (s, 1H, NH), 6.90 (d, 1H, J = 8.4 Hz, ArH), 7.35 (m, 1H, ArH), 7.43 (d, 1H, J = 4.0 Hz, ArH), 7.60 (m, 1H, ArH), 7.84 (d, 1H, J = 2.4 Hz, ArH), 8.17 (d, 1H, J = 2.0 Hz, ArH). Anal. ($C_{17}H_{15}BrN_2O_5S$) C, H, N.

***N*-Methyl-2-(5′-acetoxymethyl-2′-nitrophenylthio)-5-iodo-benzamide (12).** Acid **9** (0.19 g, 0.40 mmol) was treated with thionyl chloride (0.12 g, 1.00 mmol), as described for **10**. The crude acid chloride (0.20 g, 0.41 mmol; freshly prepared) in DCM (8 mL) was treated with methylamine hydrochloride (0.11 g, 1.63 mmol) in the presence of triethylamine (0.33 g, 3.25 mmol). The methylamide derivative (**12**) was purified by silica gel flash column chromatography (DCM/EtOAc: 8/2) to give a yellow oil (57.0 mg, 28%). ^{1}H NMR ($CDCl_3$, δ): 2.11 (s, 3H, $COCH_3$), 2.85 (d, 3H, NCH_3), 5.09 (s, 2H, CH_2O), 6.20 (s, 1H, NH), 6.90 (d, 1H, J = 8.4 Hz, ArH), 7.29 (d, 1H, J = 8.0 Hz, ArH), 7.37 (dd, 1H, J = 2.0, 8.4 Hz, ArH), 7.82 (dd, 1H, J = 2.0, 8.0 Hz, ArH), 8.07 (d, 1H, J = 1.6 Hz, ArH), 8.20 (d, 1H, J = 2.0 Hz, ArH). Anal. ($C_{17}H_{15}IN_2O_5S$) C, H, N. MS m/z 486.98 $(M + H)^+$.

***N*-Methyl-2-(5′-hydroxymethyl-2′-nitrophenylthio)-5-fluorobenzylamine (13).** To a solution of **10** (0.10 g, 0.26 mmol) in dry THF (5 mL), BH_3−THF complex (1 M soln in THF; 2.64 mL, 2.64 mmol) was added dropwise at 5 °C. The mixture was refluxed 5 h and left at room temperature 18 h. The reaction was quenched by addition of concd HCl at 0 °C and the solvent was removed under reduced pressure. To the residue, water (5 mL) was added and the mixture was refluxed for 30 min with vigorous stirring. After cooling down to room temperature, a saturated solution of Na_2CO_3 was added to neutralize the solution to pH 6∼7. The resulting aqueous solution was extracted with EtOAc. Combined organic layers were dried over Na_2SO_4, and the solvent was removed under reduced pressure. Silica gel flash column chromatography purification (DCM/MeOH: 9/1) gave **13** as a yellow oil (66.30 mg, 78%). ^{1}H NMR ($CDCl_3$, δ): 2.39 (s, 3H, NCH_3), 3.78 (s, 2H, CH_2N), 4.72 (s, 2H, CH_2OH), 6.63 (d, 1H, J = 8.4 Hz, ArH), 7.08 (m, 1H, ArH), 7.37 (m, 2H, ArH), 7.57 (m, 1H, ArH), 8.27 (d, 1H, J = 1.6 Hz, ArH). Anal. ($C_{15}H_{15}FN_2O_3S$) C, H, N. MS m/z 323.08 $(M + H)^+$.

***N*-Methyl-2-(5′-hydroxymethyl-2′-nitrophenylthio)-5-bromobenzylamine (14).** Amide (**11**; 0.15 g, 0.34 mmol) was treated with BH_3−THF (1 M soln in THF; 1.70 mL, 1.70 mmol) as described for **13**. Silica gel flash column chromatography (DCM/MeOH: 9/1) gave **14** as a yellow oil (74.27 mg, 57%). ^{1}H NMR ($CDCl_3$, δ): 2.38 (s, 3H, NCH_3), 3.77 (s, 2H, CH_2N), 4.70 (s, 2H, CH_2OH), 6.66 (d, 1H, J = 8.4 Hz, ArH), 7.34 (dd, 1H, J = 1.6, 8.0 Hz, ArH), 7.42 (d, 1H, J = 8.0 Hz, ArH), 7.50 (dd, 1H, J = 2.4, 8.4 Hz, ArH), 7.78 (d, 1H, J = 2.0 Hz, ArH), 8.25 (d, 1H, J = 2.0 Hz, ArH). Anal. ($C_{15}H_{15}BrN_2O_3S$) C, H, N.

***N*-Methyl-2-(5′-hydroxymethyl-2′-nitrophenylthio)-5-iodobenzylamine (15).** Amide **12** (53.0 mg, 0.11 mmol) was treated with BH_3−THF (1 M soln in THF; 1.09 mL, 1.09 mmol) as described for **13**. Silica gel flash column chromatography (DCM/MeOH: 9/1) gave **15** as a yellow oil (20.0 mg, 42%). ^{1}H NMR ($CDCl_3$, δ): 2.38 (s, 3H, NCH_3), 3.74 (s, 2H, CH_2N), 4.71 (s, 2H, CH_2OH), 6.67 (d, 1H, J = 8.4 Hz, ArH), 7.25 (d, 1H, J = 8.0 Hz, ArH), 7.34 (dd, 1H, J = 2.0, 8.4 Hz, ArH), 7.70 (dd, 1H, J = 2.0, 8.0 Hz, ArH), 7.97 (d, 1H, J = 2.0 Hz, ArH), 8.25 (m, 1H, ArH). Anal. ($C_{15}H_{15}IN_2O_3S$) C, H, N.

***N*-Methyl-2-(2′-amino-4′-hydroxymethylphenylthio)-5-fluorobenzylamine (16).** To a solution of **13** (59.20 mg, 0.18 mmol) dissolved in concd HCl (1.42 mL) and methanol (13 mL), $SnCl_2$ (207.0 mg) was added at 10 °C. The resulting reaction mixture was stirred at room temperature for 15 h. The solvent was evaporated to dryness and the yellow residue was taken into water. A saturated solution of Na_2CO_3 was added to adjust the pH to 6∼7. The clouded solution was extracted three times with EtOAc. The combined organic layers were dried over Na_2SO_4, and the solvent was removed under reduced pressure. Purification by silica gel flash column chromatography (DCM/MeOH: 9/1) afforded **16** as a colorless oil (18.20 mg, 34%). ^{1}H NMR ($CDCl_3$, δ): 2.50 (s, 3H, NCH_3), 3.88 (s, 2H, CH_2N), 4.39 (s, 2H, NH_2), 4.64 (s, 2H, CH_2OH), 6.72 (d, 1H, J = 8.0 Hz, ArH), 6.79 (m, 3H, ArH), 7.07 (dd, 1H, J = 2.4, 9.6 Hz, ArH), 7.35 (d, 1H, J = 8.0 Hz, ArH). Anal. ($C_{15}H_{17}FN_2OS$) C, H, N. MS m/z 293.11 $(M + H)^+$.

***N*-Methyl-2-(2′-amino-4′-hydroxymethylphenylthio)-5-bromobenzylamine (17).** Amide **14** (23.80 mg, 0.062 mmol) was treated with $SnCl_2$ (60.0 mg) as described for **16**. The desired compound **17** was obtained following purification by silica gel flash column chromatography (DCM/MeOH: 9/1) as a yellow oil (19.70 mg, 90%). ^{1}H NMR ($CDCl_3$, δ): 2.50 (s, 3H, NCH_3), 3.87 (s, 2H, CH_2N), 4.63 (s, 2H, CH_2OH), 6.71 (m, 1H, ArH), 6.80 (d, 1H, J = 1.6 Hz, ArH), 7.16 (dd, 1H, J = 2.0, 8.4 Hz, ArH), 7.36 (dd, 1H, J = 2.4, 8.0 Hz, ArH), 7.45 (d, 1H, J = 2.4 Hz, ArH). Anal. ($C_{15}H_{17}BrN_2OS$) C, H, N. MS m/z 353.03 $(M + H)^+$.

***N*-Methyl-2-(2′-amino-4′-hydroxymethylphenylthio)-5-iodobenzylamine (18).** Amide **15** (25.0 mg, 0.058 mmol) was treated with $SnCl_2$ (78.66 mg), as described for **16**. The desired compound **18** was obtained following purification by silica gel flash column chromatography (DCM/MeOH: 9/1) as a light orange oil (11.70 mg, 51%). ^{1}H NMR ($CDCl_3$, δ): 2.50 (s, 3H, NCH_3), 3.85 (s, 2H, CH_2N), 4.64 (s, 2H, CH_2OH), 6.50 (d, 1H, J = 8.4 Hz, ArH), 6.72 (dd, 1H, J = 1.2, 7.6 Hz, ArH), 6.80 (d, 1H, J = 1.6 Hz, ArH), 7.34 (d, 1H, J = 2.0 Hz, ArH), 7.37 (m, 1H, ArH), 7.63 (d, 1H, J = 2.4 Hz, ArH). Anal. ($C_{15}H_{17}IN_2OS$) C, H, N. MS m/z 401.02 $(M + H)^+$.

5-Fluoro-2-(5′-methyl-2′-nitrophenylthio)benzoic Acid (20). Compound **20** was prepared by the method described for **7**, by condensation of **19** (0.63 g, 2.90 mmol) with **4** (0.50 g, 2.90 mmol) in DMF (4 mL) in the presence of K_2CO_3 (1.20 g, 8.71 mmol) as a base. Organic layers were washed with water, dried over Na_2SO_4, and concentrated under reduced pressure. Purification by silica gel flash column chromatography (DCM/MeOH: 9/1) gave **20** as a light brown solid (0.55 g, 62%). ^{1}H NMR ($CDCl_3$, δ): 2.41 (s, 3H, CH_3), 6.97 (d, 1H, J = 8.4 Hz, ArH), 7.23 (m, 2H, ArH), 7.36 (m, 1H, ArH), 7.78 (dd, 1H, J = 3.2, 9.2 Hz, ArH), 7.93 (d, 1H, J = 1.2 Hz, ArH).

5-Bromo-2-(5′-methyl-2′-nitrophenylthio)benzoic Acid (21). Compound **21** was prepared by the method described for **7**, by condensation of **19** (1.25 g, 5.78 mmol) with **5** (0.99 g, 5.78 mmol) in DMF (10 mL) in the presence of K_2CO_3 (2.40 g, 17.36 mmol) as a base. Organic layers were washed with water, dried over Na_2SO_4, and concentrated under reduced pressure. Purification by silica gel flash column chromatography (DCM/MeOH: 9/1) gave **21** as an orange solid (1.10 g, 62%). ^{1}H NMR ($CDCl_3$, δ): 2.44 (s, 3H, CH_3), 7.06 (d, 1H, J = 8.4 Hz, ArH), 7.16 (d, 1H, J = 8.4 Hz, ArH), 7.31 (dd, 1H, J = 2.0, 8.4 Hz, ArH), 7.55 (dd, 1H, J = 2.4, 8.8 Hz, ArH), 7.88 (d, 1H, J = 1.2 Hz, ArH), 8.21 (d, 1H, J = 2.4 Hz, ArH).

5-Iodo-2-(5′-methyl-2′-nitrophenylthio)benzoic Acid (22). Compound **22** was prepared by the method described for **7**, by condensation of **19** (0.38 g, 1.78 mmol) with **6** (0.50 g, 1.78 mmol) in DMF (5 mL) in the presence of K_2CO_3 (0.74 g, 5.35 mmol) as a base. Organic layers were washed with water, dried over Na_2SO_4, and concentrated under reduced pressure. Purification by silica gel flash column chromatography (DCM/MeOH: 9/1) gave **22** as an orange oil (0.46 g, 62%). ^{1}H NMR ($CDCl_3$, δ): 2.35 (s, 3H, CH_3), 6.91 (d, 1H, J = 8.4 Hz, ArH), 7.23 (d, 1H, J = 11.60 Hz, ArH), 7.36 (dd, 1H, J = 2.0, 8.4 Hz, ArH), 7.75 (d, 1H, J = 2.0 Hz, ArH), 7.78 (dd, 1H, J = 2.0, 8.0 Hz, ArH), 8.16 (d, 1H, J = 1.6 Hz, ArH).

***N*,*N*-Dimethyl-2-(5′-methyl-2′-nitrophenylthio)-5-fluoro-benzamide (23).** To a suspension of **20** (0.54 g, 1.76 mmol) in anhydrous DCM (12 mL) were added thionyl chloride (0.52 g, 4.39 mmol) and a few drops of DMF. The reaction mixture was refluxed for 90 min under argon. The solvent was evaporated and the solid was used without further purification.

A solution of dimethylamine in tetrahydrofuran ($(CH_3)_2$NH−THF; 2.0 M soln in THF; 2.22 mL, 4.45 mmol) was added dropwise to a stirred solution of the freshly prepared acid chloride (0.29 g, 0.89 mmol) in dry THF (7 mL) at –70 °C. The reaction mixture was allowed to stand overnight at room temperature, then the solvent was removed under reduced pressure. The orange residue was extracted with EtOAc. The organic phase was washed with saturated Na_2CO_3 solution, followed by water, and the resulting organic layers were combined, dried over Na_2SO_4, and concentrated under reduced pressure. The product was purified by silica gel flash column chromatography (DCM/EtOAc: 8/2) to yield the desired compound (**23**) as an orange oil (0.27 g, 90%). ^{1}H NMR ($CDCl_3$, δ): 2.34 (s, 3H, CH_3), 2.85 (s, 3H, NCH_3), 3.02 (s, 3H, NCH_3), 6.80 (d, 1H, J = 8.8 Hz, ArH), 7.18 (m, 3H, ArH), 7.57 (m, 1H, ArH), 7.98 (d, 1H, J = 1.2 Hz, ArH). Anal. ($C_{16}H_{15}FN_2O_3S$) C, H, N.

***N*,*N*-Dimethyl-2-(5′-methyl-2′-nitrophenylthio)-5-bromo-benzamide (24).** The crude acid chloride (1.12 g, 2.89 mmol; freshly prepared) in THF (10 mL) was treated with $(CH_3)_2$NH−THF (2.0 M soln in THF; 7.24 mL, 14.48 mmol) as described for **23**. The dimethylamide derivative **24** was purified by silica gel flash column chromatography (DCM/EtOAc: 8/2) to give an orange oil (0.56 g, 49%). ^{1}H NMR ($CDCl_3$, δ): 2.35 (s, 3H, CH_3), 2.87 (s, 3H, NCH_3), 3.02 (s, 3H, NCH_3), 6.85 (d, 1H, J = 8.4 Hz, ArH), 7.20 (dd, 1H, J = 1.6, 8.0 Hz, ArH), 7.42 (d, 1H, J = 8.0 Hz, ArH), 7.56 (m, 1H, ArH), 7.57 (m, 2H, ArH), 7.98 (d, 1H, J = 1.6 Hz, ArH). Anal. ($C_{16}H_{15}BrN_2O_3S$) C, H, N.

***N*,*N*-Dimethyl-2-(5′-methyl-2′-nitrophenylthio)-5-iodo-benzamide (25).** The crude acid chloride (0.12 g, 0.28 mmol; freshly prepared) in THF (2 mL) was treated with $(CH_3)_2$NH−THF (2.0 M soln in THF; 0.69 mL, 1.38 mmol) as described for **23**. The dimethylamide derivative **25** was purified by silica gel flash column chromatography (DCM/EtOAc: 8/2) to give a yellow oil (60.0 mg, 50%). ^{1}H NMR ($CDCl_3$, δ): 2.34 (s, 3H, CH_3), 2.85 (s, 3H, NCH_3), 3.00 (s, 3H, NCH_3), 6.86 (d, 1H, J = 8.4 Hz, ArH), 7.19 (dd, 1H, J = 1.6, 8.0 Hz, ArH), 7.25 (d, 1H, J = 8.0 Hz, ArH), 7.48 (m, 2H, ArH), 7.95 (d, 1H, J = 0.8 Hz, ArH). Anal. ($C_{16}H_{15}IN_2O_3S$) C, H, N.

***N*,*N*-Dimethyl-2-(5′-bromomethyl-2′-nitrophenylthio)-5-fluoro-benzamide (26).** A mixture of **23** (0.27 g, 0.81 mmol), *N*-bromosuccinimide (0.21 g, 1.21 mmol), and AIBN (27.0 mg) was refluxed for 24 h in CCl_4 (12 mL). The solvent was removed under reduced pressure and the residue was purified by silica gel flash column chromatography using DCM/EtOAc (8/2) as eluent. Compound **26** was obtained as a yellow oil (0.15 g, 45%). ^{1}H NMR ($CDCl_3$, δ): 2.87 (s, 3H, NCH_3), 3.04 (s, 3H, NCH_3), 4.43 (s, 2H, CH_2Br), 6.88 (d, 1H, J = 8.4 Hz, ArH), 7.18 (m, 2H, ArH), 7.39 (dd, 1H, J = 2.0, 8.4 Hz, ArH), 7.60 (m, 1H, ArH), 8.23 (d, 1H, J = 2.0 Hz, ArH).

***N*,*N*-Dimethyl-2-(5′-bromomethyl-2′-nitrophenylthio)-5-bromo-benzamide (27).** Compound **24** (0.55 g, 1.39 mmol) was treated with *N*-bromosuccinimide (0.37 g, 2.09 mmol) and AIBN (16.0 mg) as described for **26**. The reaction mixture was refluxed for 18 h in CCl_4 (13 mL) and the dimethylamide derivative **27** was purified by silica gel flash column chromatography (DCM/EtOAc: 8/2) to give an orange residue (0.38 g, 57%). ^{1}H NMR ($CDCl_3$, δ): 2.87 (s, 3H, NCH_3), 3.02 (s, 3H, NCH_3), 4.43 (s, 2H, CH_2Br), 6.87 (d, 1H, J = 8.4 Hz, ArH), 7.41 (dd, 1H, J = 2.0, 8.8 Hz, ArH), 7.57 (m, 2H, ArH), 7.62 (dd, 1H, J = 2.4, 8.4 Hz, ArH), 8.22 (d, 1H, J = 2.0 Hz, ArH).

***N*,*N*-Dimethyl-2-(5′-bromomethyl-2′-nitrophenylthio)-5-iodo-benzamide (28).** Compound **25** (59.0 mg, 0.13 mmol) was treated with *N*-bromosuccinimide (35.62 mg, 0.20 mmol) and AIBN (6.0 mg) as described for **26**. The reaction mixture was refluxed for 24 h in CCl_4 (3 mL) and the dimethylamide derivative **28** was purified by silica gel flash column chromatography (DCM/EtOAc: 8/2) to give an orange oil (45.0 mg, 65%). ^{1}H NMR ($CDCl_3$, δ): 2.87 (s, 3H, NCH_3), 3.01 (s, 3H, NCH_3), 4.43 (s, 2H, CH_2Br), 6.86 (d, 1H, J = 8.4 Hz, ArH), 7.20 (d, 1H, J = 8.4 Hz, ArH), 7.39 (dd, 1H, J = 1.6, 8.0 Hz, ArH), 7.78 (m, 2H, ArH), 8.21 (d, 1H, J = 2.0 Hz, ArH).

***N*,*N*-Dimethyl-2-(5′-acetoxymethyl-2′-nitrophenylthio)-5-fluoro-benzamide (29).** A mixture of compound **26** (0.15 g, 0.36 mmol) and CH_3CO_2K (35.0 mg, 0.36 mmol) was stirred at 120 °C for 18 h in DMF (6 mL). The mixture was cooled to room temperature, poured into cold water, and extracted several times with EtOAc. The combined organic layers were washed thoroughly with water, dried over Na_2SO_4, and concentrated under reduced pressure. Silica gel flash column chromatography purification (DCM/EtOAc: 8/2) afforded **29** as a yellow oil (69.80 mg, 50%). ^{1}H NMR ($CDCl_3$, δ): 2.09 (s, 3H, $COCH_3$), 2.87 (s, 3H, NCH_3), 3.03 (s, 3H, NCH_3), 5.06 (s, 2H, CH_2O), 6.90 (d, 1H, J = 8.4 Hz, ArH), 7.16 (m, 2H, ArH), 7.36 (dd, 1H, J = 2.0, 8.4 Hz, ArH), 7.58 (m, 1H, ArH), 8.20 (d, 1H, J = 2.0 Hz, ArH). Anal. ($C_{18}H_{17}FN_2O_5S$) C, H, N. MS m/z 393.09 $(M + H)^+$.

***N*,*N*-Dimethyl-2-(5′-acetoxymethyl-2′-nitrophenylthio)-5-bromo-benzamide (30).** Compound **27** (0.37 g, 0.78 mmol) was treated with CH_3CO_2K (76.58 mg, 0.78 mmol) as described for **29**. The reaction mixture was heated at 145 °C for 20 h in DMF (5 mL) and the dimethylamide derivative **30** was purified by silica gel flash

column chromatography (DCM/EtOAc: 8/2) to give an orange oil (0.18 g, 51%). ^{1}H NMR ($CDCl_3$, δ): 2.08 (s, 3H, $COCH_3$), 2.86 (s, 3H, NCH_3), 3.01 (s, 3H, NCH_3), 5.06 (s, 2H, CH_2O), 6.91 (d, 1H, J = 8.4 Hz, ArH), 7.35 (dd, 1H, J = 2.0, 8.4 Hz, ArH), 7.43 (d, 1H, J = 8.4 Hz, ArH), 7.58 (m, 2H, ArH), 8.17 (d, 1H, J = 1.6 Hz, ArH). Anal. ($C_{18}H_{17}BrN_2O_5S$) C, H, N.

***N,N*-Dimethyl-2-(5′-acetoxymethyl-2′-nitrophenylthio)-5-iodobenzamide (31).** Compound **28** (45.0 mg, 0.086 mmol) was treated with CH_3CO_2K (8.50 mg, 0.086 mmol) as described for **29**. The reaction mixture was heated at 110 °C for 20 h in DMF (2 mL) and the dimethylamide derivative **31** was purified by silica gel flash column chromatography (DCM/EtOAc: 8/2) to give a yellow oil (22.0 mg, 51%). ^{1}H NMR ($CDCl_3$, δ): 2.09 (s, 3H, $COCH_3$), 2.87 (s, 3H, NCH_3), 3.01 (s, 3H, NCH_3), 5.07 (s, 2H, CH_2O), 6.93 (d, 1H, J = 8.4 Hz, ArH), 7.28 (d, 1H, J = 8.0 Hz, ArH), 7.36 (dd, 1H, J = 2.0, 8.4 Hz, ArH), 7.76 (d, 1H, J = 1.6 Hz, ArH), 7.80 (dd, 1H, J = 2.0, 8.0 Hz, ArH), 8.18 (d, 1H, J = 2.0 Hz, ArH). Anal. ($C_{18}H_{17}IN_2O_5S$) C, H, N.

***N,N*-Dimethyl-2-(5′-hydroxymethyl-2′-nitrophenylthio)-5-fluorobenzylamine (32).** Amide **29** (67.40 mg, 0.17 mmol) was treated with BH_3−THF complex (1 M soln in THF; 3.43 mL, 3.43 mmol) as described for **13**. Silica gel flash column chromatography purification (DCM/MeOH: 9/1) gave **32** as a yellow oil (13.20 mg, 23%). ^{1}H NMR ($CDCl_3$, δ): 2.19 (s, 6H, NCH_3), 3.49 (s, 2H, CH_2N), 4.72 (s, 2H, CH_2OH), 6.61 (d, 1H, J = 8.4 Hz, ArH), 7.05 (m, 1H, ArH), 7.33 (m, 1H, ArH), 7.46 (dd, 1H, J = 2.0, 8.4 Hz, ArH), 7.54 (m, 1H, ArH), 8.26 (d, 1H, J = 1.6 Hz, ArH). Anal. ($C_{16}H_{17}FN_2O_3S$) C, H, N.

***N,N*-Dimethyl-2-(5′-hydroxymethyl-2′-nitrophenylthio)-5-bromo-benzylamine (33).** Amide **30** (0.18 g, 0.39 mmol) was treated with BH_3−THF (1 M soln in THF; 1.98 mL, 1.98 mmol) as described for **13**. Silica gel flash column chromatography (DCM/MeOH: 9/1) gave **33** as an orange oil (0.16 g, 99%). ^{1}H NMR ($CDCl_3$, δ): 2.27 (s, 6H, NCH_3), 3.59 (s, 2H, CH_2N), 4.73 (s, 2H, CH_2OH), 6.65 (d, 1H, J = 8.4 Hz, ArH), 7.35 (dd, 1H, J = 2.0, 8.4 Hz, ArH), 7.41 (d, 1H, J = 8.4 Hz, ArH), 7.49 (dd, 1H, J = 1.6, 8.0 Hz, ArH), 7.94 (m, 1H, ArH), 8.26 (d, 1H, J = 1.6 Hz, ArH). Anal. ($C_{16}H_{17}BrN_2O_3S$) C, H, N.

***N,N*-Dimethyl-2-(5′-hydroxymethyl-2′-nitrophenylthio)-5-iodobenzylamine (34).** Amide **31** (22.0 mg, 0.044 mmol) was treated with BH_3−THF (1 M soln in THF; 0.22 mL, 0.22 mmol) as described for **13**. Silica gel flash column chromatography (DCM/MeOH: 9/1) gave **34** as a yellow oil (11.00 mg, 56%). ^{1}H NMR ($CDCl_3$, δ): 2.27 (s, 6H, NCH_3), 3.47 (s, 2H, CH_2N), 4.72 (s, 2H, CH_2OH), 6.67 (d, 1H, J = 8.4 Hz, ArH), 7.66 (dd, 1H, J = 2.0, 8.0 Hz, ArH), 7.75 (d, 1H, J = 2.0 Hz, ArH), 7.79 (dd, 1H, J = 2.0, 8.0 Hz, ArH), 8.04 (d, 1H, J = 2.0 Hz, ArH), 8.24 (d, 1H, J = 1.6 Hz, ArH). Anal. ($C_{16}H_{17}IN_2O_3S$) C, H, N.

***N,N*-Dimethyl-2-(2′-amino-4′-hydroxymethylphenylthio)-5-fluoro-benzylamine (35).** Amide **32** (13.20 mg, 0.040 mmol) was treated with $SnCl_2$ (44.27 mg) as described for **16**. The desired compound **35** was obtained following purification by silica gel flash column chromatography (DCM/MeOH: 9/1) as a colorless oil (8.40 mg, 70%). ^{1}H NMR ($CDCl_3$, δ): 2.32 (s, 6H, NCH_3), 3.56 (s, 2H, CH_2N), 4.63 (s, 2H, CH_2OH), 6.71 (dd, 1H, J = 2.0, 8.0 Hz, ArH), 6.76 (m, 1H, ArH), 6.81 (dd, 1H, J = 3.2, 8.4 Hz, ArH), 6.87 (m, 1H, ArH), 7.03 (d, 1H, J = 7.2 Hz, ArH), 7.42 (d, 1H, J = 7.6 Hz, ArH). Anal. ($C_{16}H_{19}FN_2OS$) C, H, N. MS m/z 307.12 $(M + H)^+$.

***N,N*-Dimethyl-2-(2′-amino-4′-hydroxymethylphenylthio)-5-bromo-benzylamine (36).** Amide **33** (75.0 mg, 0.19 mmol) was treated with $SnCl_2$ (0.18 g) as described for **16**. The desired compound **36** was obtained following purification by silica gel flash column chromatography (DCM/MeOH: 9/1) as a light orange oil (62.0 mg, 89%). ^{1}H NMR ($CDCl_3$, δ): 2.31 (s, 6H, NCH_3), 3.53 (s, 2H, CH_2N), 4.61 (s, 2H, CH_2OH), 6.70 (d, 1H, J = 8.0 Hz, ArH), 6.82 (m, 2H, ArH), 7.15 (dd, 1H, J = 2.0, 8.4 Hz, ArH), 7.39 (m, 2H, ArH). Anal. ($C_{16}H_{19}BrN_2OS$) C, H, N. MS m/z 367.04 $(M + H)^+$.

***N,N*-Dimethyl-2-(2′-amino-4′-hydroxymethylphenylthio)-5-iodo-benzylamine (37).** Amide **34** (21.40 mg, 0.048 mmol) was treated with $SnCl_2$ (45.0 mg, 0.20 mmol) as described for **16**. The desired compound **37** was obtained following purification by silica gel flash column chromatography (DCM/MeOH: 9/1) as an orange oil (7.20 mg, 36%). ^{1}H NMR ($CDCl_3$, δ): 2.46 (s, 6H, NCH_3), 3.65 (s, 2H, CH_2N), 4.65 (s, 2H, CH_2OH), 6.56 (d, 1H, J = 8.4 Hz, ArH), 6.72 (d, 1H, J = 8.0 Hz, ArH), 6.79 (m, 1H, ArH), 7.39 (m, 1H, ArH), 7.67 (m, 1H, ArH), 7.77 (d, 1H, J = 8.4 Hz, ArH). Anal. ($C_{16}H_{19}IN_2OS$) C, H, N. MS m/z 415.03 $(M + H)^+$.

Radiochemistry. (1) Radiosynthesis of [^{11}C]-(35). [^{11}C]-(**35**) was prepared in a manner similar to the previously reported "loop method".[43] A commercial front load HPLC injector is equipped with a commercial stainless steel loop (2 mL). A trap is connected to the load waste port of the HPLC injector to catch the untrapped [^{11}C]iodomethane. With the valve in the LOAD position, a solution of precursor **16** (0.8–1.0 mg) in DMF (70 μL) is injected slowly (5–10 s) into the clean, dry injection loop using a 100 μL syringe. The loading of the loop with precursor solution can be made at least up to 10 min before end of bombardment (EOB). The [^{11}C]iodomethane product line of the GE MicroLab methyl iodide system was inserted into the load port of the injector. [^{11}C]iodomethane, produced from $^{11}CO_2$,[24] was swept into the HPLC loop coated with precursor solution by a stream of helium gas (25 mL/min) at room temperature. Radioactivity trapped on the loop is detected by a proximal radiation detector. When radioactivity had peaked in the loop (2–3 min), the flow of helium is stopped and the reaction allowed to proceed (5 min). The contents of the loop were then quantitatively injected onto the HPLC purification column (A) by simply changing the position of the injection valve to INJECT. The semipreparative HPLC solvent was 50% absolute ethanol (abs. EtOH)/50% H_2O/0.1% triethylamine (Et_3N), and the flow rate = 5 mL/min (rt of [^{11}C]-(**35**) = 12.57 min, rt of **16** = 8.15 min). The appropriate fractions were collected and condensed via solid phase extraction (SPE) method.[44] An aliquot (0.1 mL) of the formulated solution was used to establish the chemical and radiochemical purities and specific activity of the final solution by analytical HPLC: column B, 70% MeOH/30% H_2O/0.1% Et_3N, 1 mL/min (rt of [^{11}C]-(**35**) = 3.72 min). The quality control tests showed that the final product was sterile, pyrogen-free, and contained no precursor. Further evidence for the identity of the radiolabeled product was achieved by coinjection with authentic "cold" material on column B. [^{11}C]-(**36**) and [^{11}C]-(**37**) were prepared in a similar manner: for ligand [^{11}C]-(**36**), column A, 8 mL/min (rt of [^{11}C]-(**36**) = 14.72 min, rt of **17** = 7.85 min); column B, 1 mL/min (rt of [^{11}C]-(**36**) = 5.42 min). For ligand [^{11}C]-(**37**), column A, 8 mL/min (rt of [^{11}C]-(**37**) = 12.87 min, rt of **18** = 7.60 min); column B, 1 mL/min (rt of [^{11}C]-(**37**) = 5.82 min).

(2) Solid Phase Extraction. The 2.5 mL fractions of [^{11}C]-(**35**) collected from the semipreparative HPLC column were diluted with sterile water (5 mL/fraction) and combined in one flask. After stirring, the homogeneous solution was transferred with vacuum, through a Cook line, to a C_{18} Sep Pak (previously activated with abs. EtOH (10 mL) and water (10 mL)), the eluate being directed to the waste. After two successive washings, one with saline (0.9% NaCl, 50 mL) and one with abs. EtOH (0.5 mL), all directed to the waste, the [^{11}C]-(**35**) was eluted with abs. EtOH (1.5 mL) and driven to a sterile 30 mL vial containing 0.9% NaCl solution (13.5 mL). The residue was pushed with argon through a Millipore filter (pore size 1.0 μm), followed by a smaller one (pore size 0.2 μm), to a 30 mL sterile empty vial for quality control tests and microPET nonhuman primate imaging studies. [^{11}C]-(**36**) and [^{11}C]-(**37**) were formulated in a similar manner.

(3) Log *P* Measurements. The determination of partition coefficients of radioactive compounds [^{11}C]-(**35**), [^{11}C]-(**36**), and [^{11}C]-(**37**) between 1-octanol and 0.02 M phosphate buffer at pH 7.4 was performed as reported previously.[23]

In Vitro Competition Assays. Competition assays were performed based on methods reported previously.[23–25] Cell membranes from HEK-293 cells stably expressing hSERT or hNET (gift from Dr. Randy Blakely, Ph.D., Vanderbilt University) and MDCK (Madin Darby Canine Kidney) cells stably expressing hDAT (gift from Dr. Gary Rudnick, Yale University) were used in these assays.

Cells were grown to confluency in DMEM (Dulbecco's modification of Eagles's medium) containing 10% fetal bovine serum and Geneticin sulfate and then harvested using pH 7.4 phosphate-buffered saline (PBS) containing 0.53 mM ethylenediaminetetracetic acid (EDTA) at 37 °C. Cell pellets were prepared through centrifugation at 2000 rpm for 10 min, the supernatant was decanted, and the pellets were homogenized with a Polytron PT3000 (Brinkman, Littau, Switzerland) at 11000 rpm for 12 s in 30 volumes of PBS. The resulting cell membrane suspensions were centrifuged at 43000 *g* for 10 min, the supernatants were decanted and the resulting pellets were stored at −70 °C until used in assays.

Competition assays were performed in 13 × 100 mm polystyrene tubes in a 2.0 mL final volume consisting of 1.7 mL of assay buffer, 100 μL of competing ligand in assay buffer, 100 μL of radioligand in assay buffer, and 100 μL of cell membrane suspension (corresponding to 30–70 μg protein) in assay buffer. Cell membrane pellets were characterized prior to competition assays to determine membrane concentrations that gave optimal signal while not significantly affecting the concentration of free radioligand. The cell membrane pellets were resuspended in the appropriate volume of assay buffer through brief homogenization using a Polytron PT3000. Competing ligands were assayed in triplicate at 12 concentrations ranging from 10^{-13} to 10^{-5} M. To ensure solubility, the competing ligands were dissolved in 1:1 ethanol/5 mM HCl and then serially diluted in 5 mM HCl.

For SERT assays, the assay buffer consisted of 53 mM Tris buffer, 126 mM NaCl, and 5.3 mM KCl (pH 7.9 at room temperature) and the equilibrium incubation time was 2 h at room temperature. The radioligand used for SERT assays was [^{3}H]-citalopram, obtained from Dupont NEN (Boston, MA; 3100 GBq/mmol). For NET assays, the assay buffer consisted of 53 mM Tris buffer, 320 mM NaCl, and 5.3 mM KCl (pH 7.4 at 4 °C), and the equilibrium incubation time was 4 h at 4 °C. The radioligand used for NET assays was [^{3}H]nisoxetine, obtained from Dupont NEN (3000 GBq/mmol). For DAT assay, the assay buffer consisted of 42 mM sodium phosphate buffer and 320 mM sucrose (pH 7.4 at room temperature), and the equilibrium incubation time was 1 h at room temperature. The radioligand used for DAT assays was [^{125}I]RTI-55, obtained from Dupont NEN (Boston, MA, 2200 Ci/mmol, 2.0 nM final concentration). All assays were initiated by the addition of the cell membrane suspension.

At the end of the incubation, the assays were terminated by the addition of ∼5 mL of assay buffer at 4 °C followed by rapid vacuum filtration with 3 × 5 mL washes with assay buffer at 4 °C through GF/B filters (Whatman, Inc., Clifton, NJ) presoaked in assay buffer containing 0.3% polyethyleneimine. The data from the competition curves were analyzed and K_i values calculated using GraphPad Prism software (GraphPad software, San Diego, CA). The reported K_i values are the average of at least two separate assays, each in duplicates, for each compound.

MicroPET Nonhuman Primate Studies. MicroPET imaging studies were acquired in an adult male cynomolgus monkey weighing 7.50–8.35 kg using a Concorde microPET P4 imaging system (Knoxville, TN).[24] Briefly, the microPET imaging studies were performed using 6.90–18.20 mCi of [^{11}C]-(**35**), [^{11}C]-(**36**), or [^{11}C]-(**37**) with or without injection of pharmacological doses of monoamine transporter ligands. Emission data were collected in the microPET imaging studies continuously for either 90 min after injection of [^{11}C]-(**36**) or 120 min after injection of [^{11}C]-(**35**) or [^{11}C]-(**37**) and then binned into either 18 (90 min) or 20 (120 min) time frames ranging in duration from 30 s to 10 min for analysis. Acquired emission data were subject to iterative reconstruction (OSEM, two iterations, 40 subsets) with no pre- or postfiltering to provide images with an isotropic resolution of 3 mm fwhm. For generation of time−activity curves, regions of interest (ROIs) were drawn manually based on the anatomical landmarks visible in reconstructed PET images using ASIPro software (Concorde, Knoxville, TN). The data were converted to standard uptake values (SUV). SUV were defined as the pixel value in μCi/mL multiplied by [weight of the animal (g)]/[dose (μ Ci)].

Pharmacological Displacement in Nonhuman Primates. The validity of in vivo [^{11}C]-(**35**), [^{11}C]-(**36**), and [^{11}C]-(**37**) binding to brain regions rich in SERT of a male cynomolgus monkey was assessed by their displacements by the potent selective SERT ligand *R*,*S*-citalopram.[24] *R*,*S*-Citalopram (1.5 mg/kg) was administered as a bolus over 30 s at 45 min following injection of [^{11}C]-(**35**) and at 60 min following injection of [^{11}C]-(**36**) or [^{11}C]-(**37**). Emission data were collected continuously for either 90 min after injection of [^{11}C]-(**35**) or 120 min after injection of [^{11}C]-(**36**) or [^{11}C]-(**37**). Prior to the [^{11}C]-(**35**), [^{11}C]-(**36**), or [^{11}C]-(**37**) imaging protocol, a transmission scan was obtained with a germanium-68 source for attenuation correction of the emission data. Regions of interest were drawn as described above.

Acknowledgment. This research was sponsored by the National Institute of Mental Health (R21 MH66622-01).

Supporting Information Available: Theoretical and experimental elemental analyses for compounds **16**−**18** and **35**−**37** and the actual uptake data plotted in Figures **2**, **3**, **4**, **6**, **7**, and **8**.

References

(1) Wong, E. H. F.; Sonders, S. S.; Amara, S. G.; Tinholt, P. M.; Piercey, M. F. P.; Hoffmann, W. P.; Hyslop, D. K.; Franklin, S.; Porsolt, R. D.; Bonsignoti, A.; Carfagna, N.; McArthur, R. A. Reboxetine: A pharmacologically potent, selective, and specific norepinephrine reuptake inhibitor. *Biol. Psychiatry* **2000**, *47*, 818–829.

(2) Milak, M. S.; Ogden, R. T.; Vinocur, D. N.; Van Heertum, R. L.; Cooper, T. B.; Mann, J. J.; Parsey, R. V. Effects of tryptophan depletion on the binding of [^{11}C]-DASB to the serotonin transporter in baboons: Response to acute serotonin deficiency. *Biol. Psychiatry* **2005**, *57*, 102–106.

(3) Sen, S.; Villafuerte, S.; Nesse, R.; Stoltenberg, S. F.; Hopcian, J.; Gleiberman, L.; Weder, A.; Burmeister, M. Serotonin transporter and GABA(A) alpha 6 receptor variants are associated with neuroticism. *Biol. Psychiatry* **2004**, *55*, 244–249.

(4) Deckersbach, T.; Dougherty, D. D.; Rauch, S. L. Functional imaging of mood and anxiety disorder. *J. Neuroimaging* **2006**, *16*, 1–10.

(5) Sorgi, K. L.; Maryanoff, C. A.; McComsey, D. F.; Graden, D. W.; Maryanoff, B. E. Asymmetric induction in an enammonium-iminium rearrangement. Mechanistic insight via NMR, deuterium labeling, and reaction rate studies. Application to the stereoselective synthesis of pyrroloisoquinoline antidepressants. *J. Am. Chem. Soc.* **1990**, *112*, 3567–3583.

(6) Szabo, Z.; Kao, P. F. >; Scheffel, U.; Suehiro, M.; Mathews, W. B.; Ravert, H. T.; Musachio, J. L.; Marenco, S.; Kim, S. E.; Ricaurte, G. A.; Wong, D. F.; Wagner, H. N., Jr.; Dannals, R. F. Positron emission tomography imaging of serotonin transporters in the human brain using [^{11}C](+)McN5652. *Synapse* **1995**, *20*, 37–43.

(7) Jagust, W. J.; Eberling, J. L.; Biegon, A.; Taylor, S. E.; VanBrocklin, H. F.; Jordan, S.; Hanrahan, S. M.; Roberts, J. A.; Brennan, K. M.; Mathis, C. A. Iodine-123-5-iodo-6-nitroquipazine: SPECT radiotracer to image the serotonin transporter. *J. Nucl. Med.* **1996**, *37*, 1207–1214.

(8) Meltzer, C. C.; Smith, G.; Dekosky, S. T.; Pollock, B. G.; Mathis, C. A.; Moore, R. Y.; Kupfer, D. J.; Reynolds, C. F., III. Serotonin in aging, late-life depression, and Alzheimer's disease: The emerging role of functional imaging. *Neuropsychopharmacology* **1998**, *18*, 407–430.

(9) Helfenbein, J.; Sandell, J.; Halldin, C.; Chalon, S.; Emond, P.; Okubo, Y.; Chou, Y.-H.; Frangin, Y.; Douziech, L.; Gareau, L.; Swahn, C-G.; Besnard, J.-C.; Farde, L.; Guilloteau, D. PET examination of three potent cocaine derivatives as specific radioligands for the serotonin transporter. *Nucl. Med. Biol.* **1999**, *26*, 491–499.

(10) Parsey, R. V.; Slifstein, M.; Hwang, D.-R.; Abi-Dargam, A.; Simpson, N.; Guo, N.; Van Heertum, R.; Mann, J. J.; Laruelle, M. Validation and reproducibility of measurement of 5-HT1A receptor parameters with [carbonyl-^{11}C]WAY-100635 in humans: comparison of arterial and reference tissue input functions. *J. Cereb. Blood Flow Metab.* **2000**, *20*, 1111–1133.

(11) Sandell, J.; Halldin, C.; Sovago, J.; Chou, Y. H.; Gulyas, B.; Yu, M.; Emond, P.; Nagren, K.; Guilloteau, D.; Farde, L. PET examination of [^{11}C]5-methyl-6-nitroquipazine, a radioligand for visualization of the serotonin transporter. *Nucl. Med. Biol.* **2002**, *29*, 651–656.

(12) Goodman, M. M.; Chen, P.; Plisson, C.; Martarello, L.; Galt, J.; Votaw, J. R.; Kilts, C. D.; Malveaux, G.; Camp, V. M.; Shi, B.; Ely, T. D.; Howell, L.; McConathy, J.; Nemeroff, C. B. Synthesis and characterization of iodine-123 labeled 2β-carbomethoxy-3β-(4′-((*Z*-2-iodoethenyl)phenyl)-nortropane. A ligand for in vivo imaging of serotonin

transporters by single-photon-emission tomography. *J. Med. Chem.* **2003**, *46*, 925–935.
(13) Plisson, C.; Jarkas, N.; McConathy, J.; Voll, R. J.; Votaw, J.; Williams, L.; Howell, L. L.; Kilts, C. D.; Goodman, M. M. Evaluation of carbon-11-labeled 2β-carbomethoxy-3β-[4′-((*Z*)-2-iodoethenyl)phenyl]nortropane as a potential radioligand for imaging the serotonin transporter by PET. *J. Med. Chem.* **2006**, *49*, 942–946.
(14) Plisson, C.; McConathy, J.; Martarello, L.; Malveaux, E. J.; Camp, V. M.; Williams, L.; Votaw, J. R.; Goodman, M. M. Synthesis, radiosynthesis, and biological evaluation of carbon-11 and iodine-123 labeled 2β-carbomethoxy-3β-[4′-((*Z*)-2-haloethenyl)phenyl]tropanes: Candidate radioligands for in vivo imaging of the serotonin transporter. *J. Med. Chem.* **2004**, *47*, 1122–1135.
(15) Stehouwer, J. S.; Jarkas, N.; Zeng, F.; Voll, R. J.; Williams, L.; Owens, M. J.; Votaw, J. R.; Goodman, M. M. Synthesis, radiosynthesis, and biological evaluation of carbon-11 labeled 2β-carbomethoxy-3β -(3′-((*Z*)-2-haloethenyl)phenyl)nortropanes: Candidate radioligands for in vivo imaging of the serotonin transporter with positron emission tomography. *J. Med. Chem.* **2006**, *49*, 6760–6767.
(16) Ferris, R. M.; Brieaddy, L.; Mehta, N.; Hollingsworth, E.; Rigdon, G.; Wang, C.; Soroko, F.; Wastila, W.; Cooper, B. Pharmacological properties of 403U76, a new chemical class of 5-hydroxytryptamine- and noradrenaline-reuptake inhibitor. *J. Pharm. Pharmacol.* **1995**, *47*, 775–781.
(17) Oya, S.; Choi, S. R.; Coenen, H.; Kung, H. F. New PET imaging agent for the serotonin transporter: [^{18}F]ACF (2-[(2-amino-4-chloro-5-fluorophenyl)thio-*N*,*N*-dimethyl-benzenmethanamine). *J. Med. Chem.* **2002**, *45*, 4716–4723.
(18) Shiue, G. G.; Choi, S. R.; Fang, P.; Hou, C.; Acton, P. D.; Cardi, C.; Saffer, J. R.; Greenberg, J. H.; Karp, J. S.; Kung, H. F.; Shiue, C. Y. *N*,*N*-Dimethyl-2-(2-amino-4-^{18}F-fluorophenylthio)-benzylamine (4-^{18}F-ADAM): An improved PET radioligand for serotonin transporters. *J. Nucl. Med.* **2003**, *44*, 1890–1897.
(19) Shiue, G. G.; Fang, P.; Shimazu, T.; Greenberg, J. H.; Alavi, A.; Shiue, C. Y. Synthesis of *N*,*N*-dimethyl-2-(2-amino-5-^{18}F-fluorophenylthio)benzylamine (5-^{18}F-ADAM): As a serotonin transporter imaging agent. *J. Nucl. Med.* **2003**, *44*, 185P.
(20) Huang, Y.; Bae, S.-A.; Zhu, Z.; Guo, N.; Roth, B. L.; Laruelle, M. Fluorinated diaryl sulfides as serotonin transporter ligands: Synthesis, structure−activity relationship study, and in vitro evaluation of fluorine-18 compounds as PET imaging agents. *J. Med. Chem.* **2005**, *48*, 2559–2570.
(21) Oya, S.; Kung, M.-P.; Acton, P. D.; Mu, M.; Hou, C.; Kung, H. F. A new single-photon emission computed tomography imaging agent for serotonin transporters: [^{123}I]IDAM, 5-iodo-2-((2-((dimethylamino)methyl)phenyl)thio) benzyl alcohol. *J. Med. Chem.* **1999**, *42*, 333–335.
(22) Erlandsson, K.; Sivananthan, T.; Lui, D.; Spezzi, A.; Townsend, C. E.; Mu, S.; Lucas, R.; Warrington, S.; Ell, P. Measuring SSRI occupancy of SERT using the novel tracer[^{123}I]ADAM: A SPECT validation study. *Eur. J. Nucl. Med. Mol. Imaging* **2005**, *32*, 1329–1336.
(23) Jarkas, N.; McConathy, J.; Voll, R. J.; Goodman, M. M. Synthesis, in vitro characterization, and radiolabeling of *N*,*N*-dimethyl-2-(2′-amino-4′-substituted-phenylthio)benzylamines: potential candidates as selective serotonin transporter radioligands. *J. Med. Chem.* **2005**, *48*, 4254–4265.
(24) Jarkas, N.; Votaw, J. R.; Voll, R. J.; Williams, L.; Camp, V. M.; Owens, M. J.; Purselle, D. C.; Bremner, J. D.; Kilts, C. D.; Nemeroff, C. B.; Goodman, M. M. Carbon-11 HOMADAM: A novel PET radiotracer for imaging serotonin transporters. *Nucl. Med. Biol.* **2005**, *32*, 211–224.
(25) Jarkas, N.; McConathy, J.; Votaw, J. R.; Voll, R. J.; Malveaux, E. J.; Camp, V. M.; Williams, L.; Goodman, R. R.; Kilts, C. D.; Goodman, M. M. Synthesis and characterization of EADAM: a selective radioligand for mapping the brain serotonin transporters by positron emission tomography. *Nucl. Med. Biol* **2005**, *32*, 75–86.
(26) Houle, S.; Ginovart, N.; Hussey, D.; Meyer, J. H.; Wilson, A. A. Imaging the serotonin transporter with positron emission tomography: Initial human studies with [^{11}C]DAPP and [^{11}C]DASB. *Eur. J. Nucl. Med.* **2000**, *27*, 1719–1722.
(27) Huang, Y.; Hwang, D.-R.; Narendran, R.; Sudo, Y.; Chatterjee, R.; Bae, S.-A.; Mawlawi, O.; Kegeles, L. S.; Wilson, A. A.; Kung, H. F.; Laruelle, M. Comparative evaluation in nonhuman primates of five PET radiotracers for imaging the serotonin transposters: [^{11}C]McN5652, [^{11}C]ADAM, [^{11}C]DASB, [^{11}C]DAPA, and [^{11}C]AFM. *J. Cereb. Blood Flow Metab.* **2002**, *22*, 1377–1398.
(28) Szabo, Z.; McCann, U. D.; Wilson, A. A.; Scheffel, U.; Owonikoro, T.; Mathews, W. B.; Ravert, H. T.; Hilton, J.; Dannals, R. F.; Ricaurte, G. A. Comparison of (+)-^{11}C-McN5652 and ^{11}C-DASB as serotonin transporter radioligands under various experimental conditions. *J. Nucl. Med.* **2002**, *43*, 678–692.
(29) Jarkas, N.; McConathy, J.; Ely, T.; Kilts, C. D.; Votaw, J. R.; Goodman, M. M. Synthesis and radiolabeling of new derivatives of ADAM, potential candidates as SERT imaging agents for PET. *J. Labelled Compd. Radiopharm.* **2001**, *44* (supp. 1), S204–S206.
(30) Tarkiainen, J.; Vercouillie, J.; Emond, P.; Sandell, J.; Hiltunen, J.; Frangin, Y.; Guilloteau, D.; Halldin, C. Carbon-11 labeling of MADAM in two different positions: A highly selective PET radioligand for the serotonin transporter. *J. Labelled Compd. Radiopharm.* **2001**, *44*, 1013–1023.
(31) Huang, Y.; Hwang, D.-R.; Zhu, Z.; Bae, S.-A.; Guo, N.; Sudo, Y.; Kegeles, L. S.; Laruelle, M. Synthesis and pharmacological characterization of a new PET ligand for the serotonin transporter: [^{11}C]5-Bromo-2-[2-(dimethylamino-methylphenylsulfanyl)]phenylamine ([^{11}C]DAPA). *Nucl. Med. Biol.* **2002**, *29*, 741–751.
(32) Huang, Y.; Bae, S.-A.; Zhu, Z.; Guo, N.; Hwang, D.-R.; Laruelle, M. Fluorinated analogues of ADAM as new PET radioligands for the serotonin transporter: Synthesis and pharmacological evaluation. *J. Labelled Compd. Radiopharm.* **2001**, *44* (supp. 1), S18–S20.
(33) Huang, Y.; Narendran, R.; Bae, S.-A.; Erritzoe, D.; Guo, N.; Zhu, Z.; Hwang, D.-R.; Laruelle, M. A PET imaging agent with fast kinetics: synthesis and in vivo evaluation of the serotonin transporter ligand [^{11}C]2-[2-(dimethylamino-methylphenylthio)]-5-fluorophenylamine ([^{11}C]AFA). *Nucl. Med. Biol.* **2004**, *31*, 727–738.
(34) Zhu, Z.; Guo, N.; Narendran, R.; Erritzoe, D.; Ekelund, J.; Hwang, D.-R.; Laruelle, M.; Bae, S.-A.; Huang, Y. The new PET imaging agent [^{11}C]AFE is a selective serotonin transporter ligand with fast brain uptake kinetics. *Nucl. Med. Biol.* **2004**, *31*, 983–994.
(35) Newberg, A. B.; Amsterdam, J. D.; Wintering, N.; Plössl, K.; Swanson, B. A.; Shults, J.; Alavi, A. ^{123}I-ADAM binding to serotonin transporters in patients with major depression and healthy controls: a preliminary study. *J. Nucl. Med.* **2005**, *46*, 973–977.
(36) Booij, J.; De Win, M. M. L. Brain kinetics of the new selective serotonin transporter tracer [^{123}I]ADAM in healthy young adults. *Nucl. Med. Biol.* **2006**, *33*, 185–191.
(37) Lin, K.-J.; Liu, C.-Y.; Wey, S.-P.; Hsiao, I.-T.; Wu, J.; Fu, Y.-K.; Yen, T.-C. Brain SPECT imaging and whole-body biodistribution with [^{123}I]ADAM-a serotonin transporter radiotracer in healthy human subjects. *Nucl. Med. Biol.* **2006**, *33*, 193–202.
(38) Goodman, M. M.; Jarkas, N.; Votaw, J. R.; Voll, R. J.; Purselle, D. C.; Kilts, C. D.; Bremner, J. D.; Meltzer, C. C.; Nemeroff, C. B. Initial experience of high resolution brain PET imaging of serotonin transporters (SERT) with [^{11}C]HOMADAM. *J. Nucl. Med.* **2006**, *47*, 136P.
(39) Oya, S.; Choi, S.-R.; Kung, M.-P.; Kung, H. F. 5-Chloro-2-(2′-((dimethylamino)methyl)-4′-iodophenylthio)benzenamine: A new serotonin transporter ligand. *Nucl. Med. Biol.* **2007**, *34*, 129–139.
(40) Polivka, Z.; Holubek, J.; Svatek, E.; Metysova, J.; Protiva, M. Fluorinated tricyclic neuroleptics: synthesis and pharmacology of 2-chloro-8-fluoro-4-(4-methylpiperazino)-4,5-dihydrothieno[2,3-*b*]-1-benzothiepin. *Collect. Czech. Chem. Commun.* **1981**, *46*, 2222–2233.
(41) Kalinin, A. V.; Bower, J. F.; Riebel, P.; Snieckus, V. The direct orthometallation-Ullmann connection. A new Cu(I)-catalysed variant for the synthesis of substituted diaryl ethers. *J. Org. Chem.* **1999**, *64*, 2986–2987.
(42) Jung, M. E.; Dansereau, M. K. Benzo[*H*]-1,6-naphthyridine synthesis via intramolecular Diels−Alder reactions of aryl oxazoles: Synthetic approach to 2-bromoleptoclinidinone. *Heterocycles* **1994**, *39*, 767–778.
(43) Wilson, A. A.; Garcia, A.; Jin, L.; Houle, S. Radiotracer synthesis from [^{11}C]-iodomethane: A remarkably simple captive solvent method. *Nucl. Med. Biol.* **2000**, *27*, 529–532.
(44) Lemaire, C.; Plenevaux, A.; Aerts, J.; Del Fiore, G.; Brihaye, C.; Le Bars, D.; Comar, D.; Luxen, A. Solid phase extraction−An alternative to the use of rotary evaporation for solvent removal in the rapid formulation of PET radiopharmaceuticals. *J. Labelled Compd. Radiopharm.* **1999**, *44*, 63–75.

JM0707929